A Molecular Dynamics Analysis: Effect of Colchicine on the Activation of Caspase-1

by

Nergis Günindi

A Dissertation Submitted to the

Graduate School of Sciences and Engineering

in Partial Fulfillment of the Requirements for

the Degree of

Master of Science

in

Chemical and Biological Engineering

May 24, 2017

A Molecular Dynamics Analysis: Effect of Colchicine on the Activation of Caspase-1

Koç University

Graduate School of Sciences and Engineering

This is to certify that I have examined this copy of a master's thesis by

Nergis Günindi

and have found that it is complete and satisfactory in all respects,

and that any and all revisions required by the final

examining committee have been made.

Committee Members:

BURAK ERMAN (ADVISOR)

CEM ALBAYRAK

AHMET GÜL

ÖZLEM KESKİN

SEDA KIZILEL

Date: 24.05.2017

To Başak (my sister), Gülgün (my mother), Hüseyin (my father) Günindi and to (my fiancé) Cihan Usta

ABSTRACT

Caspase-1 is a member of a family of aspartate-specific cysteine proteases. Since there is a large number of studies of caspase-1 in inflammation processes, this enzyme became an important drug target in order to prevent the disorders which are associated with caspase-1. Colchicine, which is a common drug used for Familial Mediterranean Fever and gouty arthritis disorders, inhibits caspase-1 activation, but the mechanism of inhibition is not clearly known. Procaspase-1 is activated through oligomerization in inflammasome and then becomes auto-activated. Some studies show that caspase-1 is regulated by allosteric regulation through a hydrogen bonding network passing dimer-dimer interface and has two conformational states which are controlled by active-site and allosteric-site inhibitors. In this study, colchicine is bound to dimer-dimer interface of procaspase-1 enzyme. By using Molecular Dynamics simulations, the changes of distances and correlations between residue pairs before and after colchicine bound was calculated. Since the structural changes on active site were observed after colchicine binding to allosteric site -dimer-dimer interface-, the inhibitory effect of colchicine on caspase-1 enzyme may be through the allosteric regulation. This outcome may be guide for further drug discoveries.

ÖZETÇE

Kaspaz-1 enzimi aspartik asit birimine özel sistein proteaz ailesinin bir üyesidir. Günümüzde inflamasyon sürecinde kaspaz-1 enzimi çalışmalarının artmasından dolayı, bu enzim kendisiyle ilişkilendirilen hastalıkları önlemek amacıyla önemli bir ilaç hedefi haline gelmiştir. Ailevi Akdeniz Ateşi ve gut artriti hastalıklarında kullanılan yaygın bir ilaç olan kolşisinin mekanizması tam olarak bilinmemekle birlikte kaspaz-1 enziminin aktivasyonunu engellediği düşünülmektedir. Prokaspaz-1 infalamazomda oligomerizasyonla kendiliğinden aktive olur. Bazı çalışmalar kaspaz-1'in dimer-dimer arayüzünde bir hidrojen bağ ağıyla allosterik regülasyona sahip olduğunu ve aktif ve allosterik kısımlarındaki inhibitörlerinin kontrolünde olan en az iki konformasyonel hali olduğunu gösterir. Bu çalışmada kolşisin ilacı prokaspaz-1 enziminin dimer-dimer ara yüzüne bağlanmıştır. Moleküler Dinamik simülasyonları yardımıyla, kolşisin bağlanmadan önce ve sonra, amino asit çiftleri arasındaki mesafe ve uyum değişimleri hesaplanmıştır. Kolşisinin dimer-dimer ara yüzüne bağlanmasından sonra enzimin aktif bölgesinde yapısal değişiklikler gözlemlendiği için, kolşisinin kaspaz-1 enzimi üzerindeki inhibitör etkisinin bu allosterik düzenleme aracılığıyla gerçekleşiyor olabileceği kanısına varılmıştır. Bu netice gelecekteki ilaç tasarımı ve keşifleri için bir kılavuz olabilir.

ACKNOWLEDGEMENTS

I would first like to express my deepest appreciation to my thesis advisor Prof. Dr. Burak Erman for his surveillance, mentorship and endless support from beginning to the end of my period of master study in Koç University. Without his guidance and persistent help this dissertation would not have been possible.

I would also like to thank to my thesis committee members Asst. Prof. Dr. Cem Albayrak, Prof. Dr. Ahmet Gül, Prof. Dr. Özlem Keskin and Asst. Prof. Dr. Seda Kızılel for sparing their precious time and for their helps during my study. I am really grateful for their leadings and supports.

I would like to thank dear decedent Mr. Vehbi Koç and Koç University family for giving me the opportunity to do research and widen my horizon. I also thank them for giving scholarship to complete my master degree.

I am grateful to Aysima Hacısüleyman for her endless help in my thesis study. I would also like to thank to my friends Emel Şen, Serena Muratçıoğlu, Büşra Gözde Balı and Ruth Murugi Karanja and other friends in Koç University for their endless friendship and support. Additionally, my dear friends Ece Yiğit, Kardelen Bayraktar, Saruhan Zaimoğlu, Osman Nuri Güler, Sinem Kocabaş, Leyla Yanmaz and Buşra Çolpu believed and supported me in every way during my education as good friends. Also I want to express my gratitude to Prof. Dr. Meltem Ercan for her advices and endless support as a family during my master study.

Last and most importantly, I want to thank to my mother Gülgün, my father Hüseyin and my sister Başak for their endless help and support throughout my educational life. Besides I wish to thank to my fiancé Cihan for his encouragement, endless support and patience. Without them, I could not reach where I am today. I dedicate this work to my family.

TABLE OF CONTENTS

ABSTRACT……iv

ÖZETÇE……...……...……v

ACKNOWLEDGEMENTS……vi

TABLE OF CONTENTS……vii

LIST OF TABLES……viii

LIST OF FIGURES……ix

1. INTRODUCTION……...……1
2. LITERATURE REVIEW……3
2.1. Caspase Family of Proteins……..……..……..3
2.2. Familial Mediterranean Fever (FMF) Syndrome and the Inflammasome …..……..…5
2.3. Structural Properties and Active Site of Caspase..……..…8
2.4. Activation Mechanism and Allosteric Regulation..……15
2.5. Colchicine……...……18
3. METHODS…….……20
3.1. Homology Modelling……..……20
3.2. Molecular Dynamics Simulations (MD) ……..22
3.2.1.Caspase-1……23
3.2.2.Procaspase-1……...……..24
3.2.3.Procaspase-1 + Colchicine……..26
3.3. Calculation of Fluctuations in Trajectory……27
3.4. B-factor Calculation……..……..28
3.5. Pearson Correlation Coefficient Matrix……..……..28
3.6. Calculation of the Distance Distributions between Residue Pairs……29
4. RESULTS……30
4.1. Homology Modelling Results……..30
4.2. Comparison of Calculated and Experimental B-factors……..……31
4.3. Pearson Correlation Coefficient Matrix……..……...33
5. DISCUSSION……..……36
5.1. Distance Changes between Residue Pairs……...……36
5.2. Pearson Correlation Coefficient Function……..……..46
5.3. Distance Changes in Cleavage Site……..……..48
6. CONCLUSION……...……...…….52
7. BIBLIOGRAPHY……..53

LIST OF TABLES

Table-1: Chimera Modeller Results……..30

LIST OF FIGURES

Figure 1: Mammalian Caspases……..……..……..……..4

Figure 2: Pathway of Familial Mediterranean Disease……..……..…….8

Figure 3: Solid Ribbon style Representation of Procaspase-1……..……..…….……9

Figure 4:Representation of purified form of ICE (pro-enzyme p45)… ……..……..……..……....……9

Figure 5: Representation of Nomenclature of Cleavage Sites……..……..……..……..……10

Figure 6: Solid Ribbon style Representation of Caspase-1……..……..……..……..……...…..11

Figure 7: Solid Ribbon style Representation of Caspase-1 in tetramer position……..……..……..…..12

Figure 8: Active form of a Caspase-1……..……..……..……..……..……..……..…..13

Figure 9: 1ICE caspase-1 enzyme in complex with an inhibitor……..……..……..……..……...….14

Figure 10: Active Site Pocket in Accordance with Loops……..……..……..……..……..…...15

Figure 11: Model for Allosteric Regulation with two conformational states……..……..……..……..…..17

Figure 12: Colchicine……..……..……..……..……....19

Figure 13: Sequence of Chain A of 3e4c molecule (caspase-1)… ……..……..……..……..……..….21

Figure 14: 3e4c structure with five models of missing structure in chain-A formed by Chimera 1.8.1……..…21

Figure 15: 3e4c structure with five models of missing structure in chain-B formed by Chimera 1.8.1…….22

Figure 16: Caspase-1 (pdb ID: 1ICE) and water box Representation in VMD……..23

Figure 17: Caspase-1 (pdb ID: 1ICE) Representation in VMD……..24

Figure 18: Procaspase-1 (pdb ID: 3E4C (without C285A mutation)) and Water Box Representation in VMD…25

Figure 19: Procaspase-1 (pdb ID: 3E4C (without C285A mutation)) Representation in VMD…….25

Figure 20: Procaspase-1 (pdb ID: 3E4C (without C285A mutation)-Colchicine Complex and Water Box Representation in VMD……...26

Figure 21: Procaspase-1 (pdb ID: 3E4C (without C285A mutation)-Colchicine Complex in VMD…….27

Figure 22: B factor Comparison for Procaspase-1……..32

Figure 23: B factor comparison for Caspase-1……32

Figure 24: Pearson Coefficient Matrix of Procaspase-1 enzyme (from 126th to 404th residue)……..34

Figure 25: Pearson Coefficient Matrix for Procaspase-1-Colchicine Complex (from 126th to 404th residue)……35

Figure 26: Active Site Region and the Significant Residues in Chain A with CPK Representation……..37

Figure 27: CPK representation of Cys285 and Cys237 residues……38

Figure 28: Probability Density Function of Distances between Cys285 and His237 residue pair…….38

Figure 29: CPK representation of Arg179, Thr180 and Arg341 residues……...39

Figure 30: Probability Density Function of Distances between Arg341 and Arg179 residue pair…….40

Figure 31: Probability Density Function of Distances between Arg341 and Thr180 residue pair…….……40

Figure 32: CPK representation of Asp336 and Arg383 residues……41

Figure 33: Probability Density Function of Distances between Asp336 and Arg383 residue pair…….42

Figure 34: Representation of Some significant residues in active caspase-1 (pdb Id: 1ICE) with a tetrapeptide inhibitor……...43

Figure 35: CPK representation of Arg179, Asp336, Arg341 and Arg383 residues (This conformation is from the last one-tenth of the time trajectory.)……..……43

Figure 36: Probability Density Function of Distances between Asp336 and Arg341 residue pair…….44

Figure 37: Probability Density Function of Distances between Arg341 and Arg383 residue pair…….44

Figure 38: Probability Density Function of Distances between Arg179 and Asp336 residue pair…….45

Figure 39: Demonstration of Negative Correlations in A chain of Procaspase-1……..…….……47

Figure 40: Demonstration of Negative Correlations in A chain of Procaspase-1-colchicine Complex……48

Figure 41: Probability Density Function of Distances between His237 and Asp297 residue pair…….49

Figure 42: Probability Density Function of Distances between His237 and Asp316 residue pair…….49

Figure 43: Probability Density Function of Distances between Cys285 and Asp297 residue pair…….50

Figure 44: Probability Density Function of Distances between Cys285 and Asp316 residue pair…….50

Chapter 1

1. INTRODUCTION

The caspase-1 enzyme, which is also named as the interleukin-1β converting enzyme (ICE), is a member of caspase family, which catalytically depends on a cysteine and specific for aspartic acid in activation [1]. Since it is associated with the IL-1β and IL-18 induced inflammation in the human body, it has become an important drug target that may enable the treatment of many disorders. Kinetic studies which will be explained in detail in Literature Review section show that the enzyme has allosteric regulation and binding of inhibitors to active site changes allosteric binding regions. The same affect is valid for the opposite situation. In the light of this study, activation of caspase-1 can be controlled with allosteric site inhibitors.

Colchicine is an effective and common drug for the treatment of Familial Mediterranean Fever (FMF) disease. It is an auto-inflammatory disease which is caused by the mutation of a protein called pyrin [2]. Since caspase-1 is responsible for inflammation and controls the secretion of inflammatory cytokines, caspase-1 is related to FMF disease thereby may be affected by colchicine. In this study, the aim is to observe conformational changes in the active site of the caspase-1, when colchicine drug is bound to dimer-dimer interface which is the region connected to allosteric network [3].

In Chapter-2, literature review is given which includes background information for caspase-1, its family of proteins, its activating complex (inflammasome), structural properties and active site of caspase-1, activation mechanism and allosteric regulation through the enzyme. Also details for the colchicine (drug) and the Familial Mediterranean Fever (FMF) Disease were given.

In Chapter-3, methods are given for the model and simulations. Details of homology modelling part (via Chimera) and Molecular Dynamics Simulations were explained (via NAMD, VMD). Homology modelling which are applied for the missing parts of pdb structure of caspase-1 and simulations for inactive, active and colchicine-bound states of caspase-1 were performed.

Also the calculations of b-factor, fluctuations in trajectory and Pearson Correlation Coefficient matrix were shown with equations. The details of each analysis were explained in Chapter-3.

In Chapter-4, results are given which were determined by using the methods in Chapter-3. The homology modelling results were calculated by Chimera whereas the distance changes between residue pairs were calculated by using MATLAB which transforms data from the trajectory of Molecular dynamics simulations.

In Chapter-5, the results which were obtained in Chapter-4 were compared to each other and literature. Distance changes among important residue pairs in active site were determined and Gaussian normal distributions of the pairs during the trajectory were shown.

In Chapter-6, conclusions of this study and future directions are given.

Chapter 2

2. LITERATURE REVIEW

2.1 Caspase Family of Proteins

The caspase family of proteins consists of members, which are cysteine-dependent aspartic acid-specific proteases. Caspase-1 was the first discovered member of this family [4].

Caspases are responsible for apoptosis and inflammation. Apoptosis- , i.e. programmed cell death, in which unwanted or function-disrupted cells goes into the process of dying, [5, 6], while inflammation is known as the cellular response of living tissues to any kind of damage in the body or pathogens.

The caspase enzyme family consists of 15 mammalian members and is classified in three groups: inflammatory caspases or group-I caspases (caspases-1, -4, -5, -12, -13, -14), initiator caspases or apoptosis caspases or group-II caspases (caspases-2, -8, -9, -10) and effector or executioner caspases (caspases-3, -6, -7) [7-10] (Figure 1).

Caspases whose substrates are inflammatory cytokines that are the main characters in inflammation are classified as inflammatory caspases [11]. They have Caspase Recruitment Domains in their N-terminus (Figure 1).

Initiator and executioner caspases are involved in apoptosis. Initiator caspases have long pro-domains, which are larger than 90 amino acids and are capable of activating themselves (Figure 1). They provoke the following multi-stage caspase activation by activating executioner caspases [12]. They may have either Death Effector Domain (DED) or Caspase Recruitment Domain (CARD) in their pro-domains. Executioner caspases have 20-30 amino acids in their pro-domains; their proteolytic cleavage reactions are performed by initiator caspases [13]. They are activated by cleavage of the linker regions between their small and large subunits [14-16].

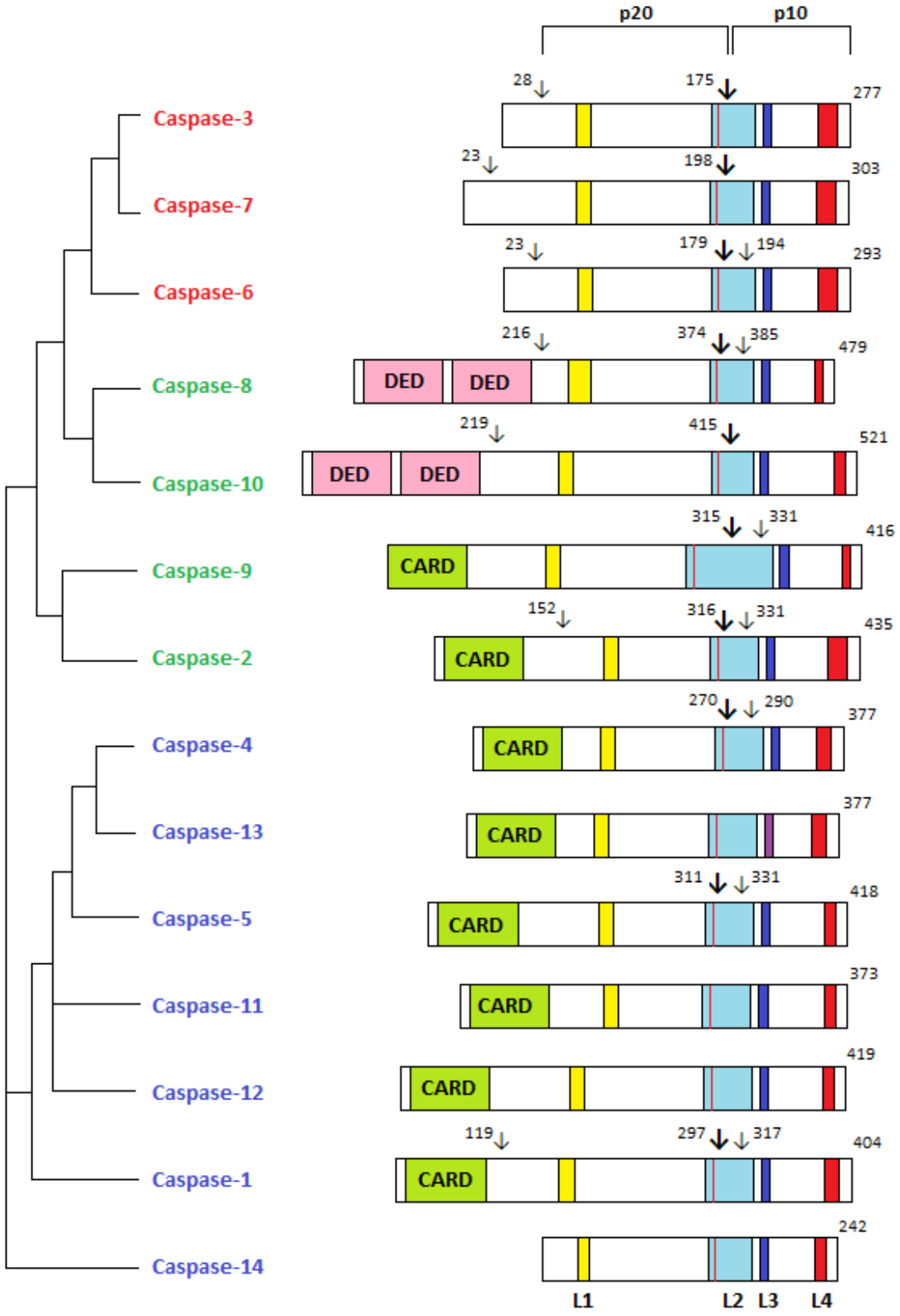

Figure 1: Mammalian Caspases (caspases-11, -12, -13 are not human origin.) In the figure, the type of enzyme, first activation cleavage sites, pro-domains –the domains before p20 subunits-, loops, and their catalytic residues are indicated with colors and arrows. Initiator caspases are

labeled in green, while the executioner caspases are indicated with red and inflammatory caspases are shown in blue. Large arrows correspond to the first cleavage regions, which is between large and small subunits, while small arrows indicate other second and third cleavage sites. The cysteine (Cys) residue, which is the catalytic residue of all caspases, is shown with a red line in the p20 subunit. At the bottom of Figure 1, the loops of substrate binding groove -L1, L2, L3, L4- are indicated which will be explained in the following sections [13].

CARD and DED which are known as the types of Death Domains (DD) [17] are important regions for the activation of caspases in vivo [18, 19]. When these CARD or DED domains approach to similar domains, cleavage reactions takes place which initiates inflammation or apoptosis. For example, initiator caspases bind to each other by using CARD domains and apoptosis process starts. If the CARD domains of inflammatory caspases come into close proximity, inflammation takes place. [13, 20, 21].

This section focuses on the similarities and differences within the caspase protein family. So, group-I and group-II caspases have similar activation mechanisms, but they initiate different biochemical pathways [22]. Even the caspases have different subgroups and are responsible for a different process from each other, zymogen latency is conserved which means the presence of an inactive enzyme that needs to be activated [8, 23].

2.2 Familial Mediterranean Fever (FMF) Syndrome and the Inflammasome

The immune system has two components, which are innate and adaptive immune system. Upon infection, the cells of innate immune system assemble and prepare to fight. The cells secrete cytokines which trigger inflammation. This system defends against harmful stimuli by sensing conserved pathogen- and danger- associated molecular patterns (PAMPs and DAMPs) through its pattern-recognition receptors (PRR) [24-26]. In hereditary auto-inflammatory disorders, mutations in the related genes of innate immune system result in dysregulated

production of specific pro-inflammatory cytokines, such as IL-1β or IL-18 as if there are endogenous danger signals or exogenous pathogenic stimuli [2].

Familial Mediterranean Fever (FMF) is an auto-inflammatory disease which induces recurrent attacks of fever, abdominal pain associated with peritonitis, chest pain associated with pleuritis, joint inflammation (arthritis), skin rashes or chronic complications such as secondary amyloidosis [24, 26-28]. FMF disorder is common in Mediterranean basin, mostly affecting Jews, -Turks, Arabs and Armenians [23, 28, 29]. The disease begins frequently before the age of 20, and its severity changes according to the mutations of the related gene [30].

This disorder is caused by the uncontrolled activation of the innate immune system. The mutation related to this disorder is in the MEFV gene which is located in chromosome 16p (in the short arm) [26]. The MEditerranean FeVer gene (MEFV) codes for the pyrin protein. This protein has a role in the multiprotein inflammasome complex, which is responsible for production of pro-inflammatory cytokines IL-1β and IL-18 [23]. So MEFV gene mutation induces a mutated pyrin production which affects the pro-inflammatory cytokine production.

Interleukin-1β (IL-1β) – a pro-inflammatory cytokine secreted by activated macrophages, is first produced as an inactive pro-Interleukin-1β (pIL-1β) protein in its 33kDa precursor state [31-33]. Upon activation by proteolytic cleavage, it causes inflammation and expression of pro-inflammatory genes [34]. It is activated when the 33kDa inactive precursor is cleaved into 17kDa IL-1β [35-38]. Upon proteolytic cleavage by caspase-1, it is processed into its active form [19]. Since caspase-1 is responsible for the IL-1β activation, it is the most important factor in innate immunity and inflammation processes [7]. Besides interleukin processing which results in inflammation and cytokine maturation, caspase-1 is also responsible for induction of pyroptosis and prodomain-mediated NF-KB activation [20]. Pyroptosis is known as pro-inflammatory programmed cell death by activation of caspase-1, whereas NF-KB activation refers to controlling transcription of DNA and cytokine production [39].

The inflammasome is an oligomer composed of proteins responsible for inflammation and therefore caspase activation. NLR (Nod-like receptor) and TLR (Toll-like receptor) protein family is two types of PRRs and components of the inflammasome [34]. NALPs are the largest subfamily in NLR protein family from NALP1 to NALP14 [34]. In FMF, NLRP3 or NALP3 inflammasome activates caspase-1 [24]. The NALP3 inflammasome, which is responsible for FMF, is composed of ASC, procaspase-1, NLRP3 and cardinal proteins (Figure 2).

The NLRP3 protein has a carboxy-terminal Leucine Rich Repeat domain (LRR), a Nucleotide binding oligomerization domain (NACHT), and an amino terminal effector domain which can be a pyrin domain (PYD) or CARD. The LRR domain is responsible for sensing the PAMPs [2]. After activation, these inflammasomes oligomerize through their NACHT domains, and their CARD domains bind to the CARD domain of pro-caspase-1 [40]. Therefore, NLRs lacking CARD domains have to connect adaptor proteins such as ASC through their PYD domains [41]. ASC has a CARD and a PYD [42]. Through its CARD, ASC can bind to procaspase-1. After other procaspase-1 enzymes are brought together with the help of cardinal proteins, proximity-induced auto-proteolysis occurs, and caspase-1 becomes activated [2, 11, 23, 25].

In the pathway of the disease, after the danger signals are sensed, NLRP3 inflammasome is formed [21]. Caspase-1 is activated, and p20 and p10 subunits are released which will be explained in detail in the following sections. Since mutated pyrin molecules bind less p10 and p20 subunits than WT pyrin, the p10-p20 subunits which cannot bind to pyrin form active caspase-1 heterodimer. [34, 43]. The activated caspase-1 then does two things: (1) it converts pro-IL-1β to IL-1β, and (2) it cleaves pyrin at the residue Asp330. The N terminal fragment of the cleaved pyrin then induces NF-KB activation. The mutation causing FMF diseases occurs in B30.2 domain of pyrin protein [23]. Figure 2 demonstrates the pathway of disease. The process on the left side with WT pyrin protein does not produce any pro-inflammatory cytokines.

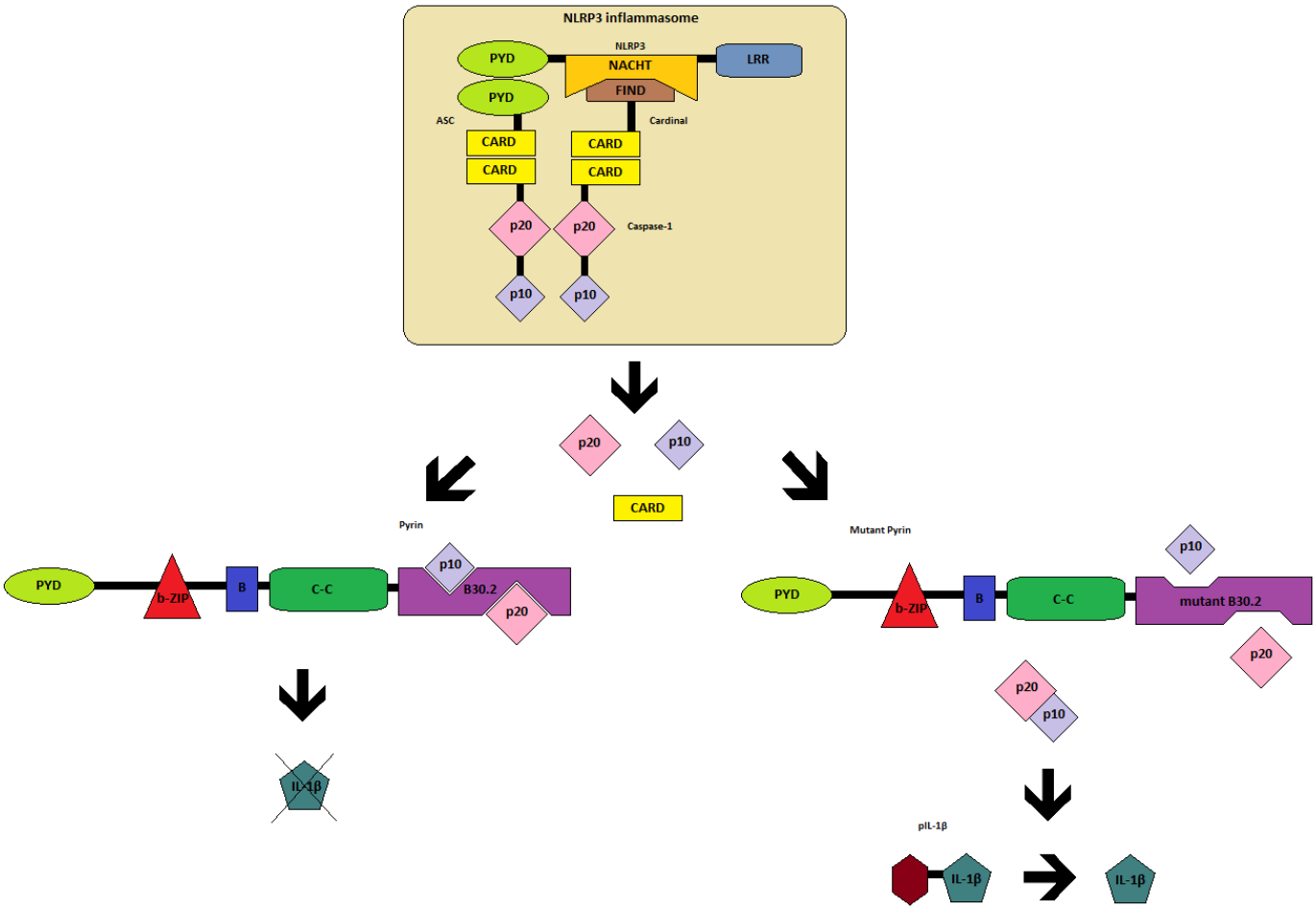

Figure 2: Pathway of Familial Mediterranean Disease [23]

2.3 Structural Properties and Active Site of Caspase-1

Procaspase-1 – the inactive form of caspase-1- has a pro-peptide, one large subunit, one small subunit and one linker region. After the proteolytic cleavage on specific aspartic acid residues, the pro-peptide –which is a 119-residue CARD- and the 18-residue linker region between the subunits are removed, and the enzyme becomes activated (Figure 3) [1, 20].

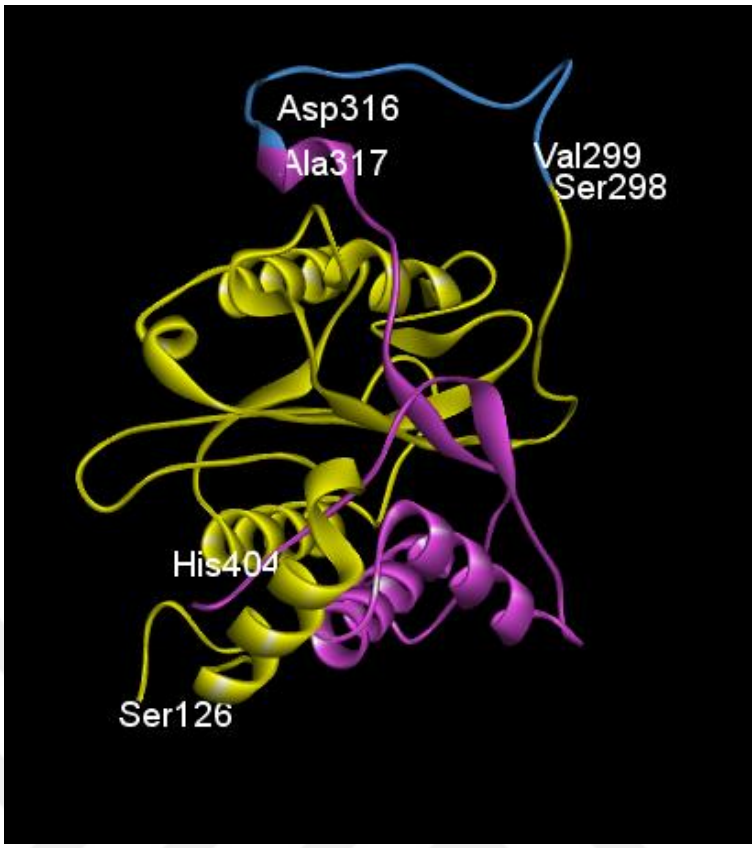

Figure 3: Solid Ribbon style Representation of Procaspase-1. (P20 subunit which is shown in yellow consists of the residues from 126 to 298 while p10 subunit which involves the residues from 317 to 404 is demonstrated in purple color. The 18-residue linker region is shown in blue color from 299th to 316th residue. This structure does not include pro-peptide. (pdb ID:3E4C-A chain))

Figure 4:Representation of purified form of ICE (pro-enzyme p45) In the figure, 5' and 3' the sequences are shown with lines. Here, 5' indicates N-terminus whereas 3' is known as C terminus of the residue [44].

The cysteine protease caspase-1 has specificity for aspartic acid residues at the P1 position of the substrate [45, 46]. The general nomenclature of cleavage site positions of the substrate was defined by Schechter and Berger, 1967-1968. In Figure 5, the position of the substrate where cleavage occurs is between P1-P1'. They specified the amino acid residues in a substrate in the N-terminal direction as P1, P2, P3, P4 etc., while the residues in the C-terminal direction are specified as P1', P2', P3', P4' etc. (Figure 5) [47]. So, for caspase-1, the bond between Asp (P1) and the following X residue (P1') should be cleaved.

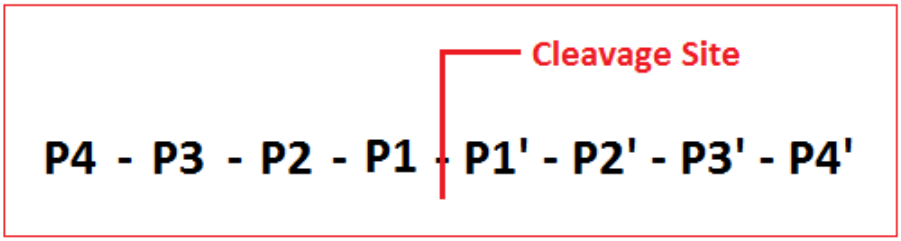

Figure 5: Representation of Nomenclature of Cleavage Sites [47]

The subunits of caspase-1 are formed by the cleavage at four Aspartate residues, which are in between Asp103-Ser104, Asp119-Asn120, Asp297-Ser298 and Asp316-Ala317 (Figure 4). The activated structure is a homodimer, which consists of two of these subunits derived from a common 45 kDa precursor (p45) (Figure 4, 7) [8, 35, 45, 48]. The smaller of the two subunits has a relative molecular mass of 10 kDa referred to as p10 (residues 317-404), and the larger subunit has a relative molecular mass of 20 kDa referred to as p20 (residues 120-298) (Figure 6) [1, 8, 45, 48]

Active and mature caspases are dimers of two heterodimers each composing of p10 and p20 units -(p20)2/(p10)2 tetramer- defined in the preceding paragraph (Figure 7) [1, 7, 8, 45, 48]. In the tetrameric form, there is a cleft in the homodimer-homodimer interface [45]. The homodimers

interact through water-mediated and hydrophobic interactions [49]. According to the crystallographic studies by Gu et al. the structure of Caspase-1 is determined as a tetramer in the crystal lattice (Figure 7) [45].

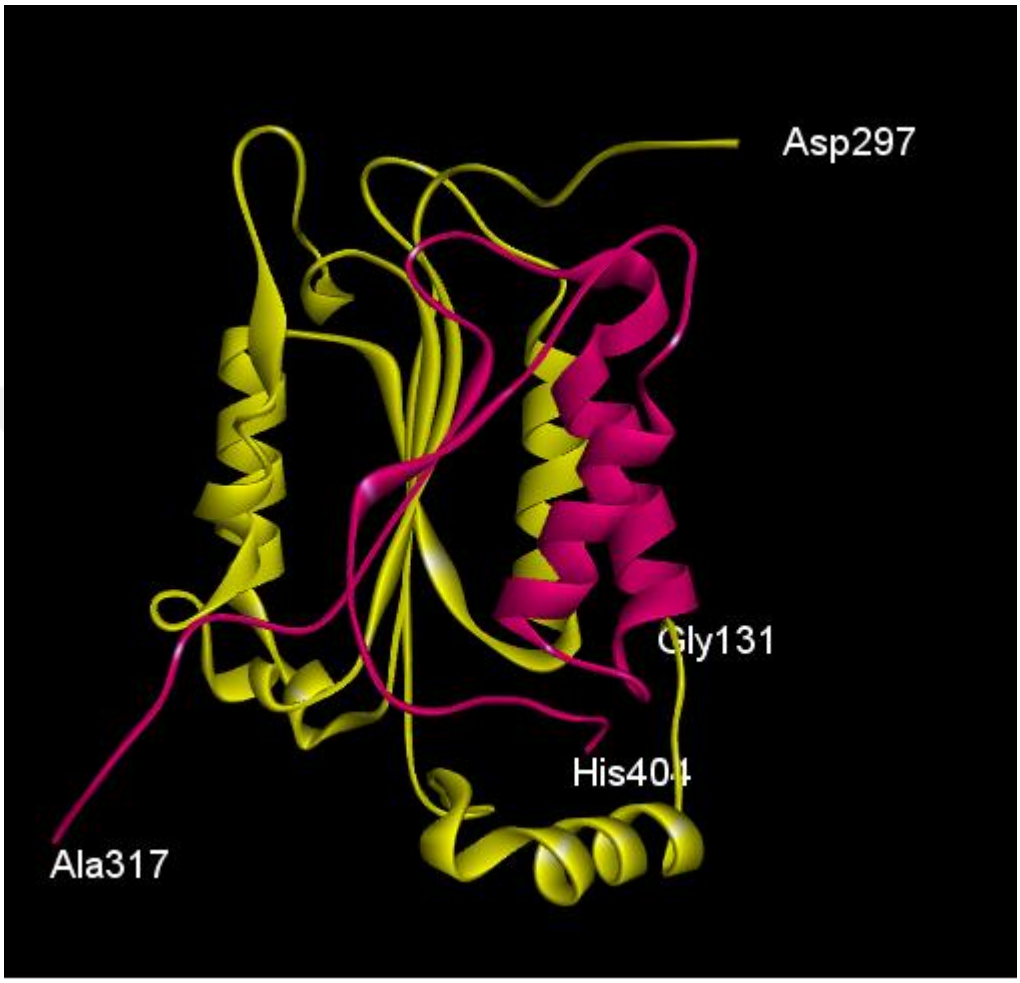

Figure 6: Solid Ribbon style Representation of Caspase-1. (P20 subunit which is shown in yellow involves the residues from 131 to 297 while p10 subunit which involves the residues from 317 to 404 is demonstrated in pink color. (pdb ID:1ICE))

Each heterodimer –p20/p10 complex- has six anti-parallel-stranded β sheet and the β sheets in two heterodimers are surrounded by five α -helices. The heterodimers, which are in compact cylinder shapes, are located as a head-to-tail configuration. Thus the active site of each heterodimer opposes each other [20] (Figure 7). Also, active site of each dimer faces the linker region of other dimer which should be cleaved for activation.

According to sequence comparison analysis of caspase-1 between different species, p10 subunit is more conserved than p20 subunit, which has homology value of 81% and 59%, respectively. Dimer-dimer interface involves mostly the residues from p10 subunit –from 318 to 322 and from 386 to 396- and thirteen of them are conserved [35, 50].

Figure 7: Solid Ribbon style Representation of Caspase-1 in tetramer position. (Pink chains correspond to p20 subunits, while p10 subunits are shown in blue color. (pdb ID:3E4C))

Each unit contains one active site, and this active binding pocket of the enzyme contains residues from both of the subunits. Cys285 is known as the catalytic site nucleophile, whereas

residues 283-285 and 236-238 in p20 subunit and residues from 338 to 343 in p10 subunit are located in this active binding region [48].

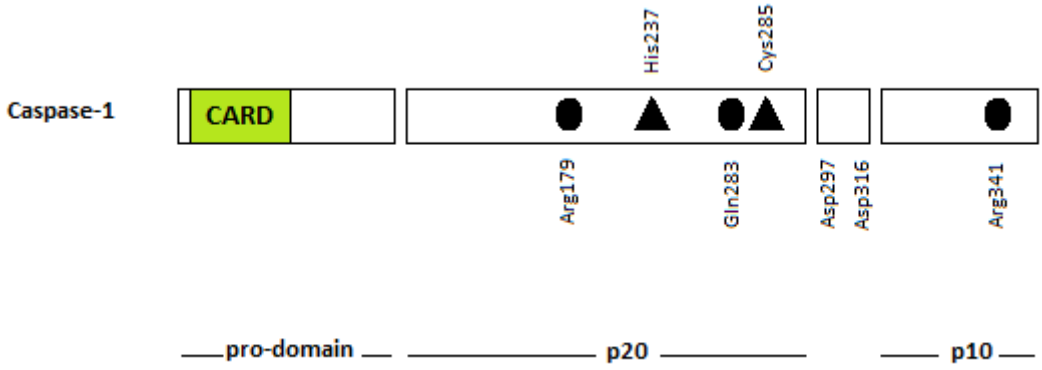

Figure 8: Active form of a Caspase-1[51]

In the active site of caspase-1, Cys285 and His237 form a catalytic dyad and they are responsible for the cleavage reaction of the enzyme [35, 45]. In Figure 8 they are shown with triangles. A thiol-containing substrate forms a covalent bond with the Sulphur atom of Cys285, while His237 forms a hydrogen bond with the oxyanion of the substrate [35].

Arg179 and Arg341 are important residues, since they interact with P1 Asp residue through H bonding (figure 8). When either Arg179 or Arg341 is mutated, the activity of the enzyme is inhibited [45].

Some residues, which are not located at the active site of the enzyme, like Glu390 and Arg391 – located in the p10 dimer-dimer interface- have effects on caspase-1 activity. Since Glu390 and Arg391 are opposed to each other in the tetramer position of the enzyme, they make a salt bridge between dimers. This bond stabilizes the enzyme in tetramer position which is the active form of the enzyme; therefore it is important for auto-processing of ICE [45]. Gu and Wu et al. applied different mutations to residues in the dimer-dimer interface and determined that especially R391E mutant has negative effects on activity. They suggested that oligomerization is required for auto-processing [45, 52].

Another significant residue which is located in the substrate binding pocket is Arg341. Amor and Yaliraki et al. performed a Markov transient analysis to detect the important regions connected to the active site [48]. According to the analysis they determined that salt bridge between Asp336 and Arg383 may retain the inactive conformation, since the breakage of this bond increases the signaling through the protein. Asp336 is known to stabilize the L3 loop, which contains Arg341, whereas the L4 loop, which includes the Arg383 residue, stabilizes the L3 loop [1]. So breakage of the Asp336-Arg383 salt bridge may affect entire dynamics of the enzyme [48]. Also hydrogen bond interaction between Arg341 and Thr180 is important for Arg341 to stabilize its position in the binding pocket [48].

Other important residues in caspase-1 activation are Arg179 and Gln283, which are responsible for aspartate recognition of substrate in P1 position [35].

Catalytic groove in caspase-1 enzyme is surrounded by L1, L2, L3 and L4 loops [13, 53]. These loops are shown in caspase-1, which is in complex with an aldehyde inhibitor (pdb ID: 1ICE) in Figure 9.

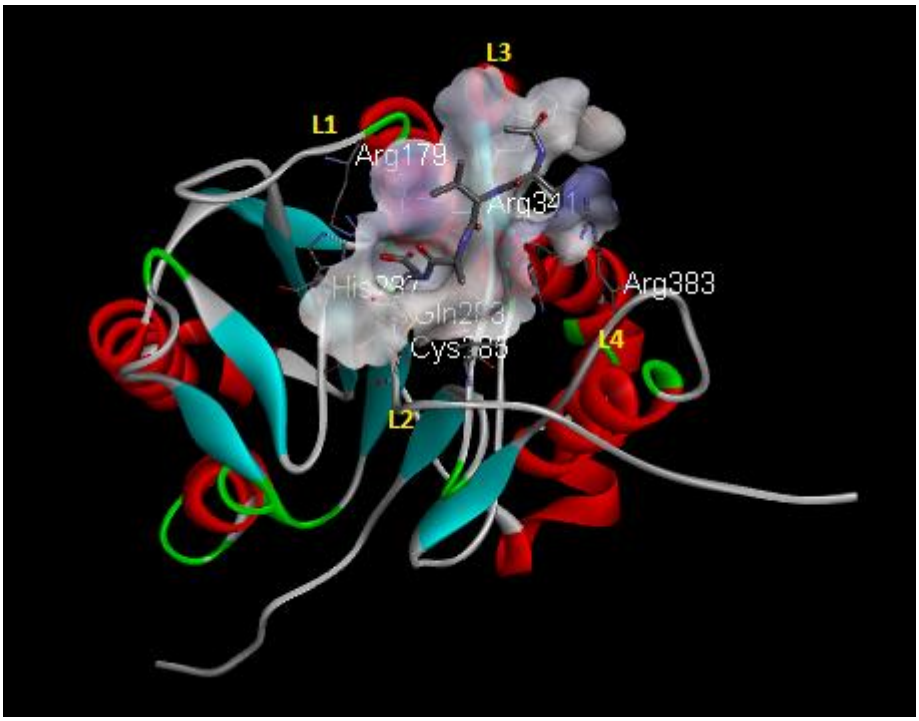

Figure 9: 1ICE caspase-1 enzyme in complex with an inhibitor [35].

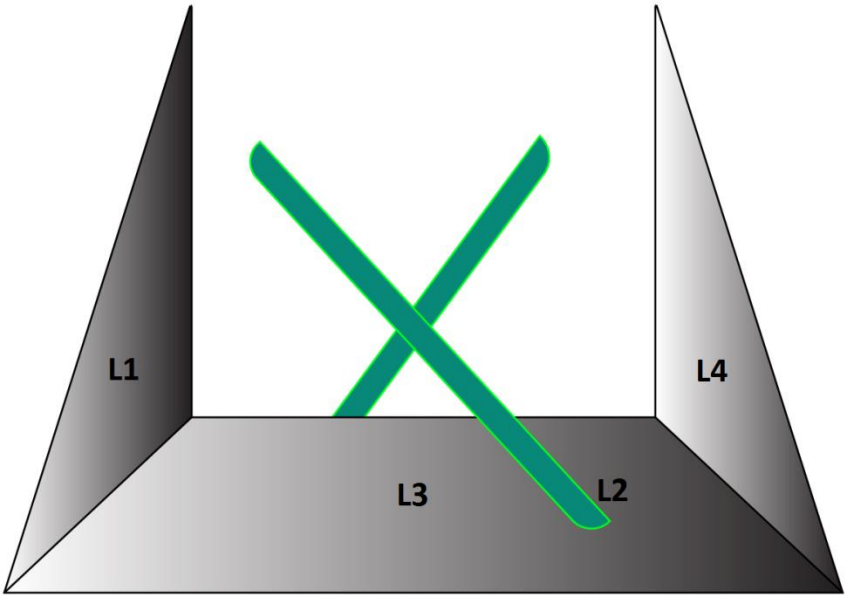

Figure 10: Active Site Pocket in Accordance with Loops [13]

Figure 10 shows a visual representation of the active site pocket of caspase-1 with loops. According to the studies, the active site pocket is on L3 loop and between the L1 and L4 loops. Cys285 in the L2 loop stabilizes this site for catalysis. L3 loop is stabilized by Asp336 and Arg341 in the L3 loop makes hydrogen bonds with substrate. Also, Arg179 and Arg383 are in the L1 and L4 loops, respectively, which make hydrogen bonds with the substrate (Shi, 2002).

2.4 Activation Mechanism and Allosteric Regulation

Caspase-1 is found in cells as a catalytically inactive monomeric zymogen called procaspase-1 (Figure 2), and is processed into its active form through dimerization and auto-proteolysis [24].

Caspase-1 exists as a monomer under physiological concentrations. However, when it reaches proteolytic maturation, it is dimerized. Steady-state Kinetic Modelling by Datta et al. showed that binding of substrate both supports the heterodimer formation and increases the substrate binding efficiencies in the other monomers, referred to as substrate-induced dimerization and substrate-induced activation, respectively [54].

According to kinetic experimental studies by Thornberry et al., after dilution, the enzyme loses its activity when tetramer dissociates into inactive subunits [54]. As explained in the previous sections, most of the residues in the dimer-dimer interface are conserved. Also, mutation of these residues causes significant changes on conformation and activity. The dimer-dimer interface encompasses an area of ≈5,200 A^2. To conclude all of these determinations, the enzyme should be a tetramer when activated [55].

Cross linking studies for protein-protein interactions propose that at low concentrations, active caspase-1 stays in monomeric form [56].This result also supports the idea that oligomerization should occur before auto-proteolysis [57]. According to Elliot et al., the first cleavage occurs at the Asp297 residue in C-terminal of the p20 subunit, which is also the N-terminal of the linker region between subunits. The Asp residue in one heterodimer is cleaved by Cys285 and His237 catalytic residues in another opposing heterodimer. Asp316 is then cleaved which causes the linker region to be detached from the enzyme (Figure 3). These reactions show that caspase-1 should possess oligomerization before auto-proteolysis and auto-activation [7, 58].

Caspase-1 has a property, which affects its activation mechanism. Allosteric regulation is a regulation of an enzyme by binding a small effector molecule or inhibitor to an enzyme's site other than its active site or an enzyme which involves cooperativity between different binding regions [3]. This binding affects dynamics of the protein and results in large conformational changes in some enzymes such as caspase-1 [59].

According to crystallographic studies, caspases have at least two conformational states [60]. One of them is the on-state in which the active site is occupied by a ligand. In the off-state, the active site is empty or the dimer-dimer interface, which is ≈15 A° away from the active site, is occupied by an allosteric ligand [61]. When an active-site ligand is bound to the enzyme, the binding of allosteric-site ligand is inhibited (Figure 11) [61]. Binding of ligands into different sites of enzyme shifts the equilibrium which is shown in Figure 11 [3].

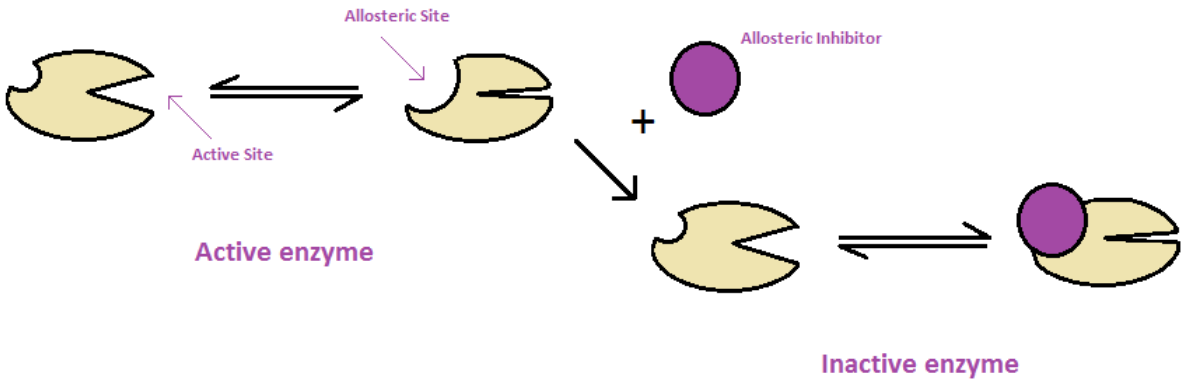

Figure 11: Model for Allosteric Regulation with two conformational states [3]

X-ray crystallography data of caspase-1 showed that the enzyme is a dimeric protease, with different crystal structures for the ligand-free and ligand-bound states. Studies by D. Datta et al. show that the enzyme can be held in the off-state by binding of an inhibitor compound to dimer interface (Figure 11). So substrate-induced dimerization may be controlled by an allosteric circuit between the dimer interface and active sites of the enzyme [54].

The X-ray structures showed that the allosteric regulation through two conformational states may be controlled by 9 side chains of 9 amino acids. These side chains control 21 hydrogen bonds, which affect the change of states and represent an allosteric network which bridges two active sites. According to the alanine scanning mutation studies in Datta et al. 2008, one of the most important interactions is the salt bridge between Arg286 and Glu390. In this analysis, the importance of a residue's side chain in activity can be determined, and only four of nine chains are found to be significant for the activity of caspase-1. Datta et al. 2008 showed that the breaking of salt bridge between Arg286 and Glu390 causes 100- to 200- fold reduction in catalytic efficiency [61].

Scheer et al. 2006 applied the disulfide trapping method to observe the allosteric circuit in caspase-1. In this study, the interaction between a library of ≈8,000 thiol-containing molecules and the cysteine residue in central cavity of caspase-1 enzyme (Cys331) was examined by the tethering method [62, 63]. During the structural and kinetic analysis of allosteric site mutants,

Scheer et al. 2006 demonstrated that the Hill coefficient of the enzyme is 1.5, which is then reduced to 1.0 when the Glu390 residue is mutated to Alanine (E390A). Since the Hill coefficient is a term that shows the interaction between ligand binding sites, this reduction indicates the significance of interaction between Glu390 and a central water on the allosteric circuit. This study reinforced allosteric regulation; that is, substrate binding on one active site enhances the catalytic activity on the second site of the enzyme [62]. Also Datta and McClendon et al. showed that binding of one site increases the catalytic activity on the second active site by 10-fold, thereby indicating strong positive cooperativity within the enzyme [54].

2.5 Colchicine

Since caspase-1 is a key player in the inflammation process in the body, it also comprises a significant drug target in order to treat the related periodic fever syndromes such as FMF.

Colchicine -*N*-[(7*S*)-1,2,3,10-Tetramethoxy-9-oxo-5,6,7,9-tetrahydrobenzo[*a*]heptalen-7-yl]acetamide-(Figure 12) is a known and widely used drug for the treatment of FMF disease [64]. It is produced naturally by *Colchicum autumnale* species [27].

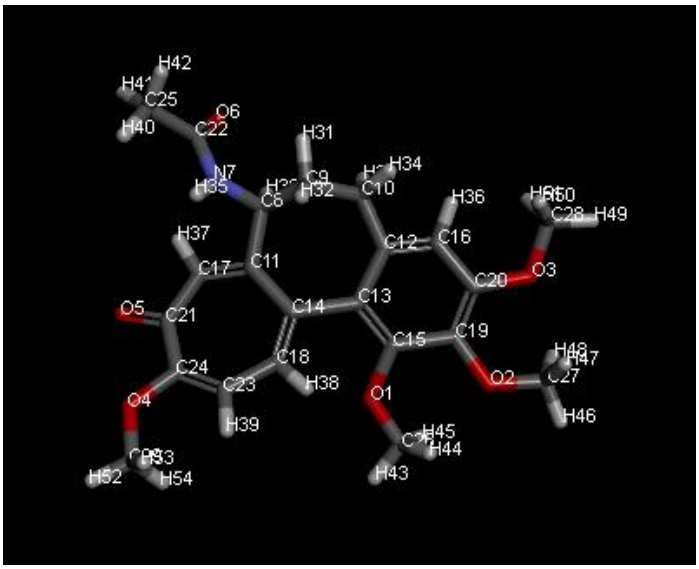

Figure 12: Colchicine

According to the studies during the last 45 years, it was observed that colchicine prevents development of attacks of pain in specific parts of the body due to FMF [64]. Wilson et al. (1994) determined non-competitive inhibitors, which binds the catalytic residue at dimer-dimer interface. Since there is an allosteric regulation through a Hydrogen bonding network in the enzyme, drugs which may bind at the dimer-dimer interface are promising for the future drug design of FMF [55]. Also, drug discovery for the active site pocket has a disadvantage for docking drug-like compounds, since they need to be long enough to engage the catalytic residues at the cleft [62, 65]. Small inhibiting molecules can be used for drug design in the dimer-dimer interface in order to control the activation mechanism of enzyme. [3, 14, 66].

The mechanism of action of colchicine in FMF is not completely understood. Although it is known to bind tubulin and prevent elongation of microtubules, it may also have a specific effect on inflammasome activation [27, 43, 67]. In this study, the aim is to understand the effect of colchicine in dimer-dimer interface on the dynamics of caspase-1. By predicting a mechanism with colchicine, the source of its inhibitory effects may be understood or new drugs may be discovered and then developed in further analysis.

Chapter 3

3. METHODS

3.1 Homology Modelling

Models of procaspase-1 structure are created by using the software Chimera 1.8.1. Three dimensional structure of procaspase-1 is formed by completing the missing parts of the crystal structure whose pdb ID is 3e4c. In Figure 13, amino acid sequence of chain A of caspase-1 is given, where red framed parts correspond to missing parts in the crystal structure. The location of the missing residues V-G-V-S-G-N-L-S is in between the large and small subunits, linker region whose cleavage is required for activation of the enzyme (Figure 13). The non-terminal missing structure, which is modelled by Chimera 1.8.1 contains eight residues which are Val299, Gly300, Val301, Ser302, Gly303, Asn304, Leu305 and Ser306. In order to refine the missing structure and remodel the loops, five models were generated and standard loop modelling protocol was followed (Figure 14). The same procedure was applied for the chain B (Figure 15).

Chimera 1.8.1 gives z-DOPE (normalized Discrete Optimized Protein Energy) scores, which are atomic distance-dependent statistical scores [68]. This score is based on the calculations of non-interacting atoms in a sample native structure. DOPE method designates models with lowest ΔRMSD which is root mean square deviation –methods for measuring the distance between two atoms-. [69]. This method is known as the most reliable method for designing the most definite models and derived by Shen and Sali [68]. According to the results, poor models have positive z-scores, whereas negative values give more accurate models [68].

```
3e4c.pdb (#0) chain A 103 QSQGVLSSFPAPQAVQDNPAMPTSSGSEGNVKLCSLEEAQRIWKQKSAEI
3e4c.pdb (#0) chain A 153 YPIMDKSSRTRLALIICNEEFDSIPRRTGAEVDITGMTMLLQNLGYSVDV
3e4c.pdb (#0) chain A 203 KKNLTASDMTTELEAFAHRPEHKTSDSTFLVFMSHGIREGICGKKHSEQV
3e4c.pdb (#0) chain A 253 PDILQLNAIFNMLNTKNCPSLKDKPKVIIIQAARGDSPGVVWFKDSVGVS
3e4c.pdb (#0) chain A 303 GNLSLPTTEEFEDDAIKKAHIEKDFIAFCSSTPDNVSWRHPTMGSVFIGR
3e4c.pdb (#0) chain A 353 LIEHMQEYACSCDVEEIFRKVRFSFEQPDGRAQMPTTERVTLTRCFYLFP
3e4c.pdb (#0) chain A 403 GH
```

Figure 13: Sequence of Chain A of 3e4c molecule (caspase-1) (Sequence is the same in chain B of 3e4c.)

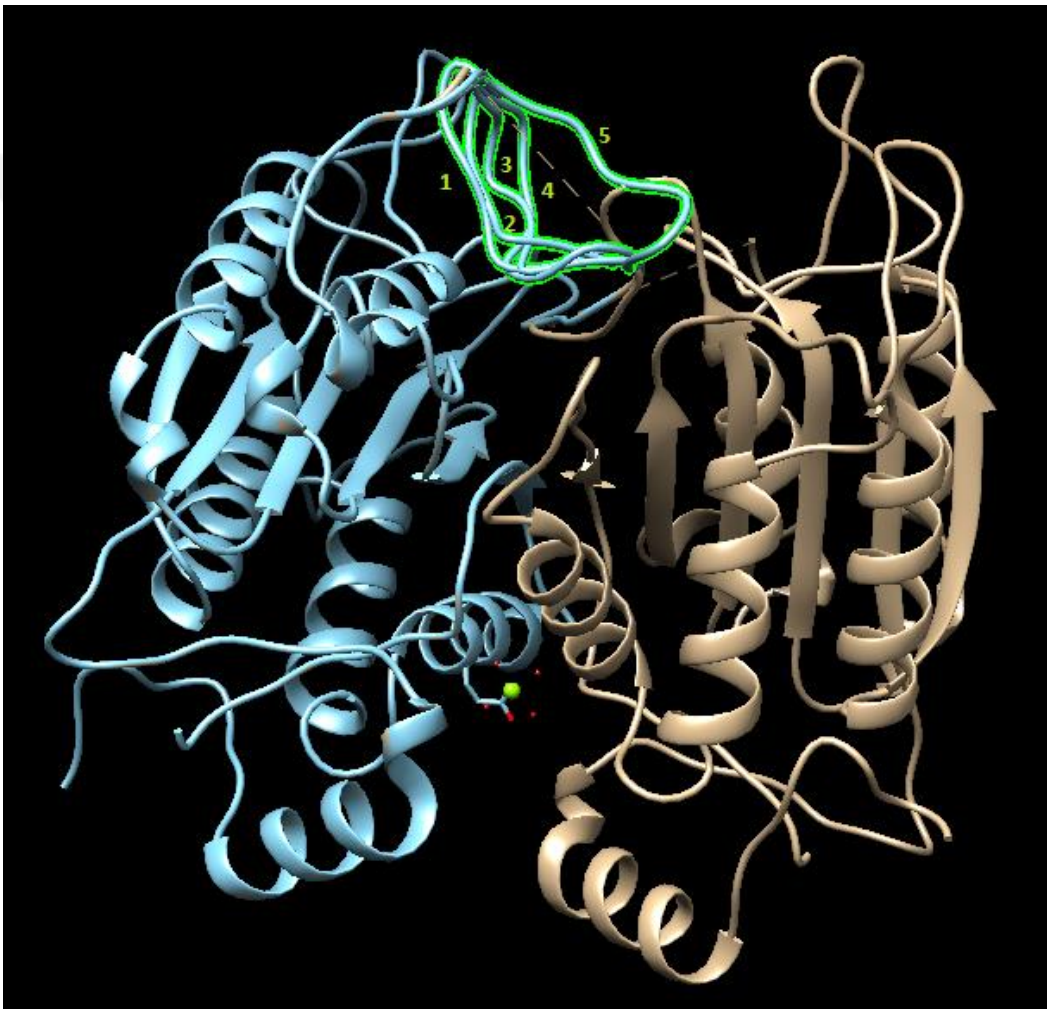

Figure 14: 3e4c structure with five models of missing structure in chain-A formed by Chimera 1.8.1.

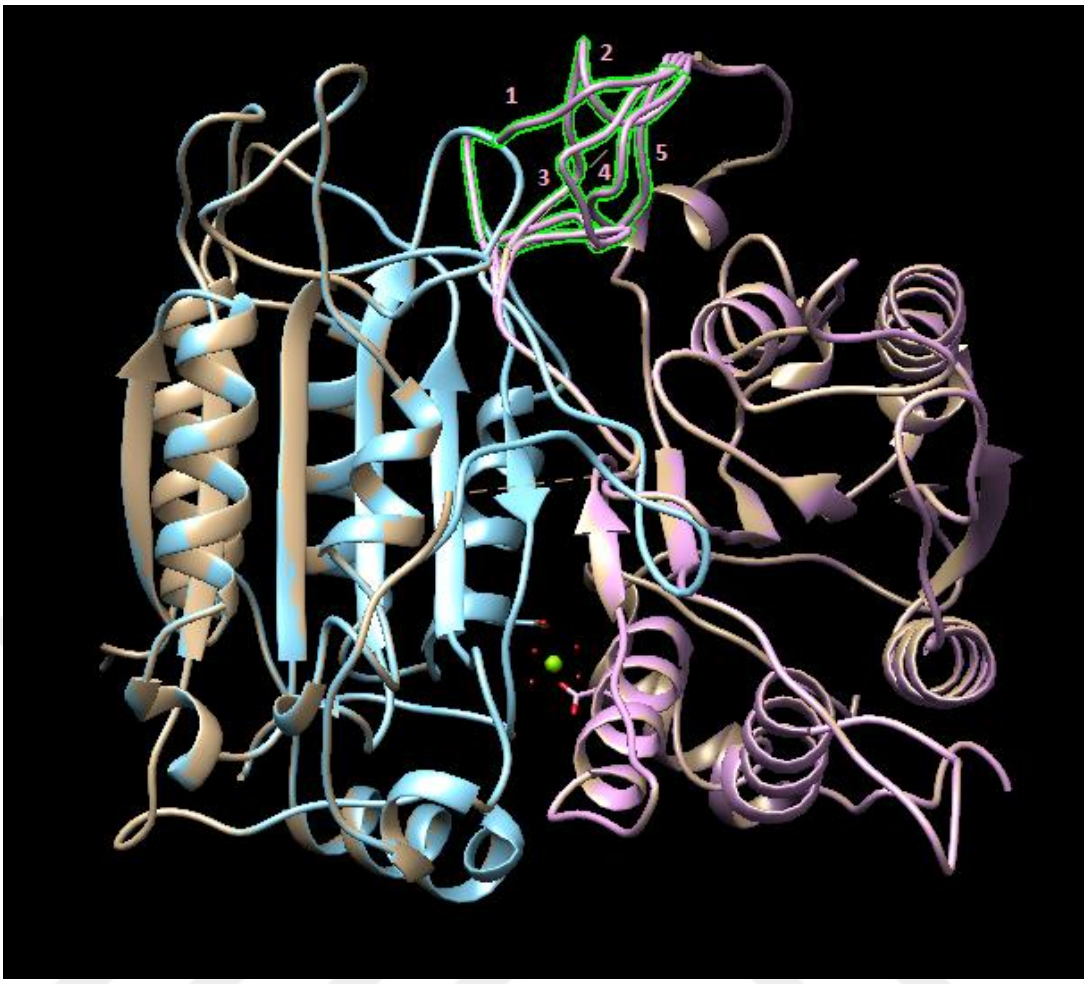

Figure 15: 3e4c structure with five models of missing structure in chain-B formed by Chimera 1.8.1.

3.2 Molecular Dynamics Simulations (MD)

Molecular Dynamic simulations were performed by using NAMD program, whereas VMD molecular graphics software was used for trajectory analysis [70]. Canonical ensemble was applied in which the temperature is constant and there is energy exchange [71, 72]. Trajectories are obtained from Molecular Dynamics simulations which are performed for 50,000,000 steps. Since one time step takes 2 femtosecond, the simulation gave a 100 nanosecond-long trajectory. The simulations were performed for procaspase-1, caspase-1 and procaspase-1-colchicine complex.

Since DCD frequency of simulation is 5000 and the number of steps is 50,000,000, the frame number in trajectory became 10,000. In this trajectory, with equal spacing, 1000 frames were used for further calculations. The coordinates of the all carbon alpha atoms in the protein were saved for 1000 chosen frames. This procedure was applied for each case.

3.2.1 Caspase-1

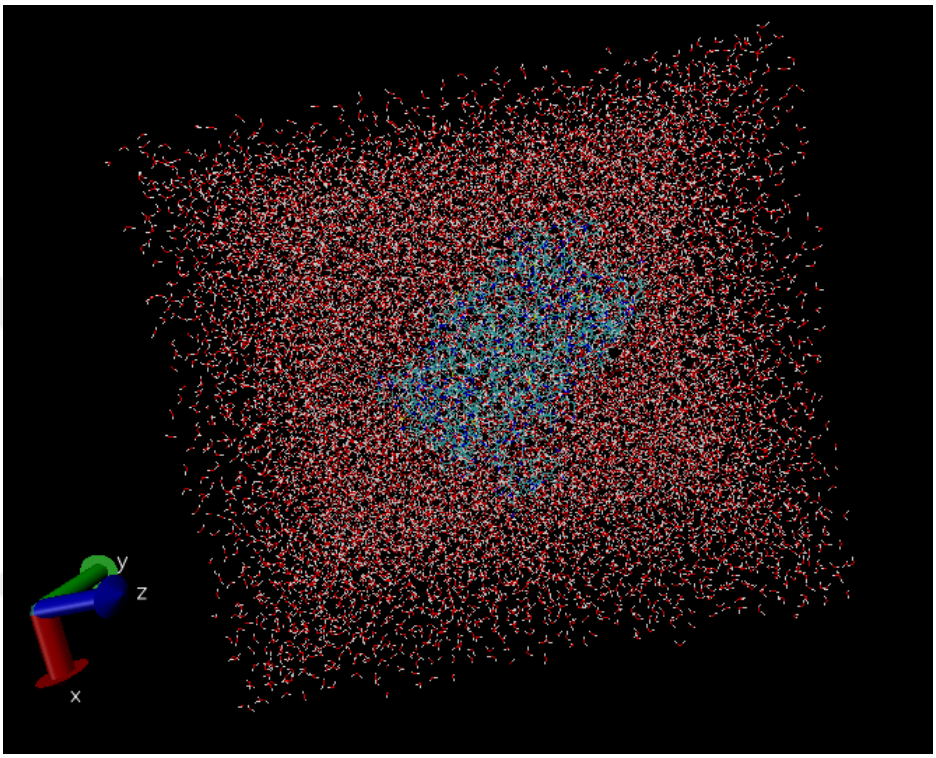

Figure 16: Caspase-1 (pdb ID: 1ICE) and water box Representation in VMD

Figure 16 demonstrates the water-box and caspase-1 together. 1ICE pdb structure was used, and simulations were performed only for one chain (one heterodimer). The crystal structure has 255 amino acids and consists of p20 and p10 subunit only. In Figure 17 only activated caspase-1 enzyme was shown in CPK representation style.

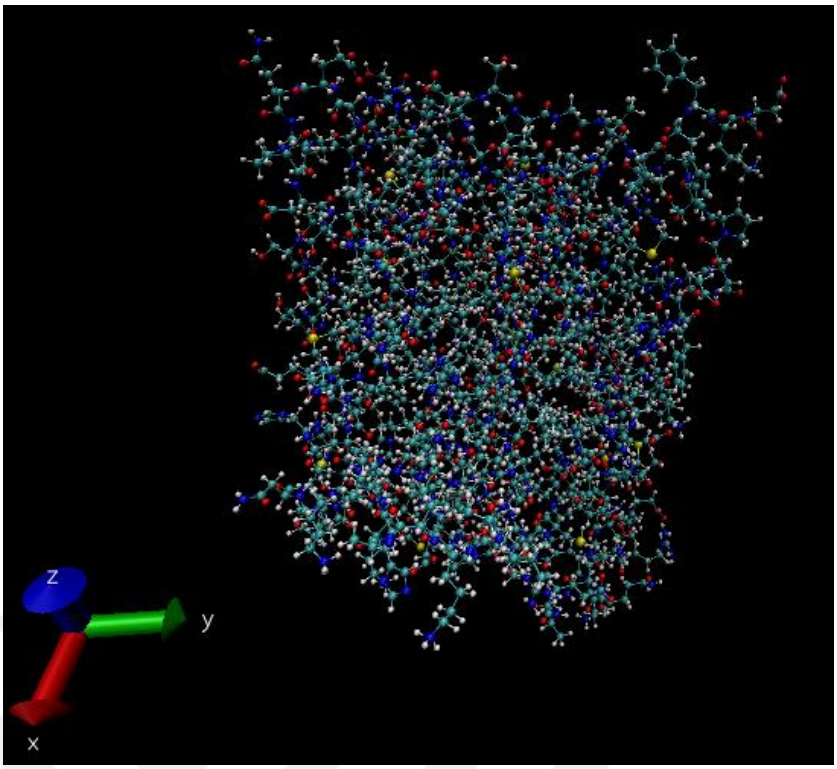

Figure 17: Caspase-1 (pdb ID: 1ICE) Representation in VMD

3.2.2 Procaspase-1

Procaspase-1 structure in tetramer position was demonstrated with water box in Figure 18. 3E4C pdb structure was used, but Ala285 was mutated back to Cys285 which is the wild type condition of enzyme. The crystal structure has 556 amino acids with the completed linker region. Again, procaspase-1 enzyme was demonstrated in CPK style in Figure 19.

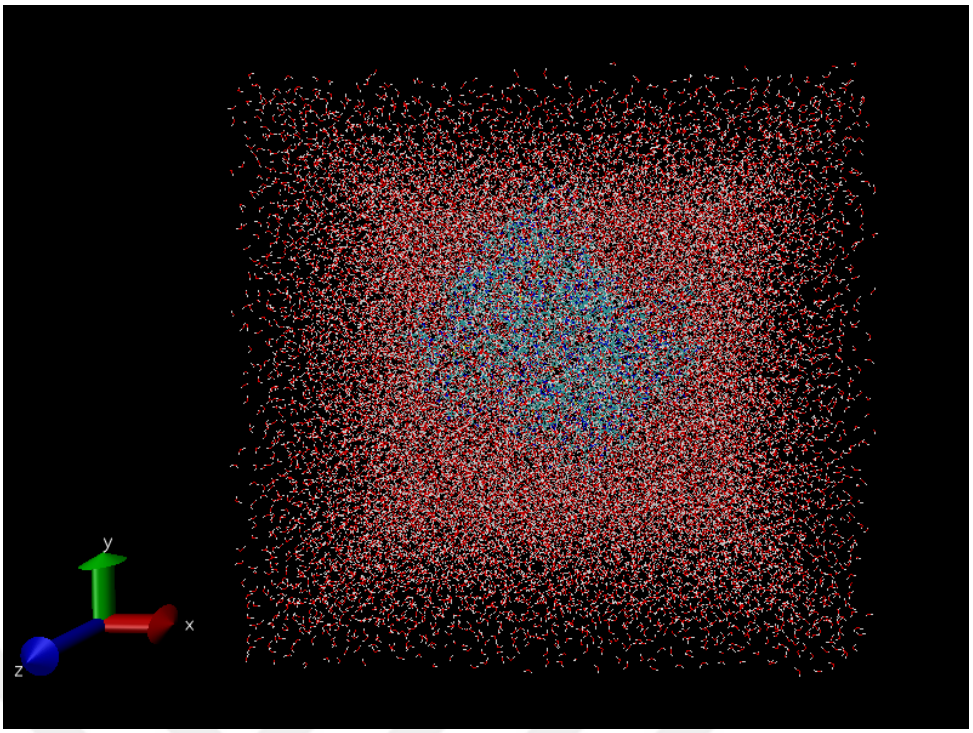

Figure 18: Procaspase-1 (pdb ID: 3E4C (without C285A mutation)) and Water Box Representation in VMD

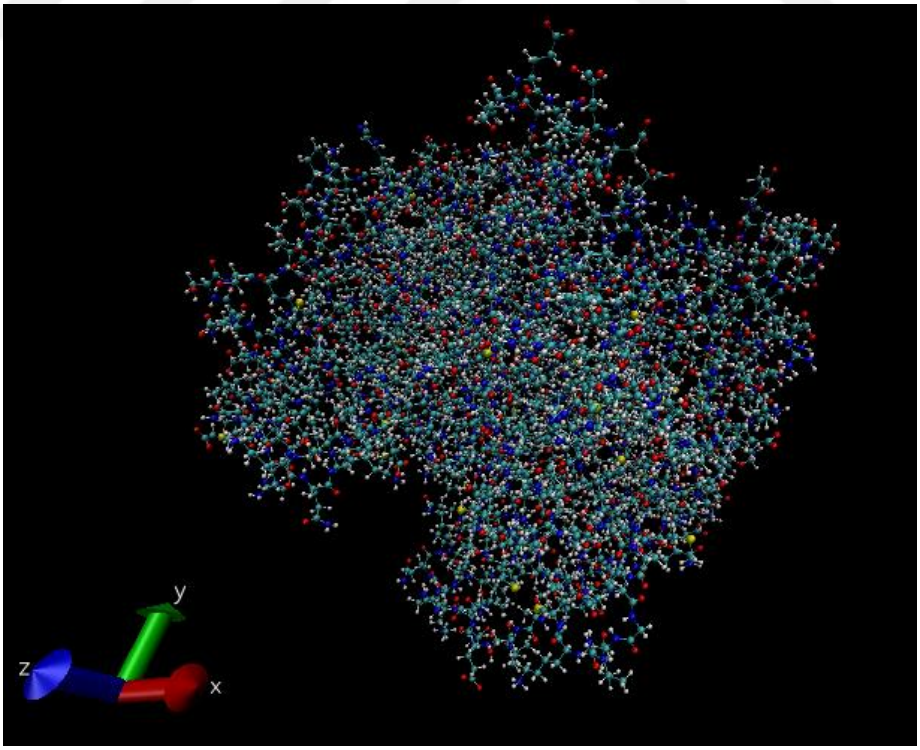

Figure 19: Procaspase-1 (pdb ID: 3E4C (without C285A mutation)) Representation in VMD

3.2.3 Procaspase-1 + Colchicine

Procaspase-1-colchicine complex with water box was shown in Figure 20, but colchicine is more distinguishable in Figure 21 seen in beads representation with light blue color between two heterodimers. The same procaspase-1 structure was used for the analysis with colchicine.

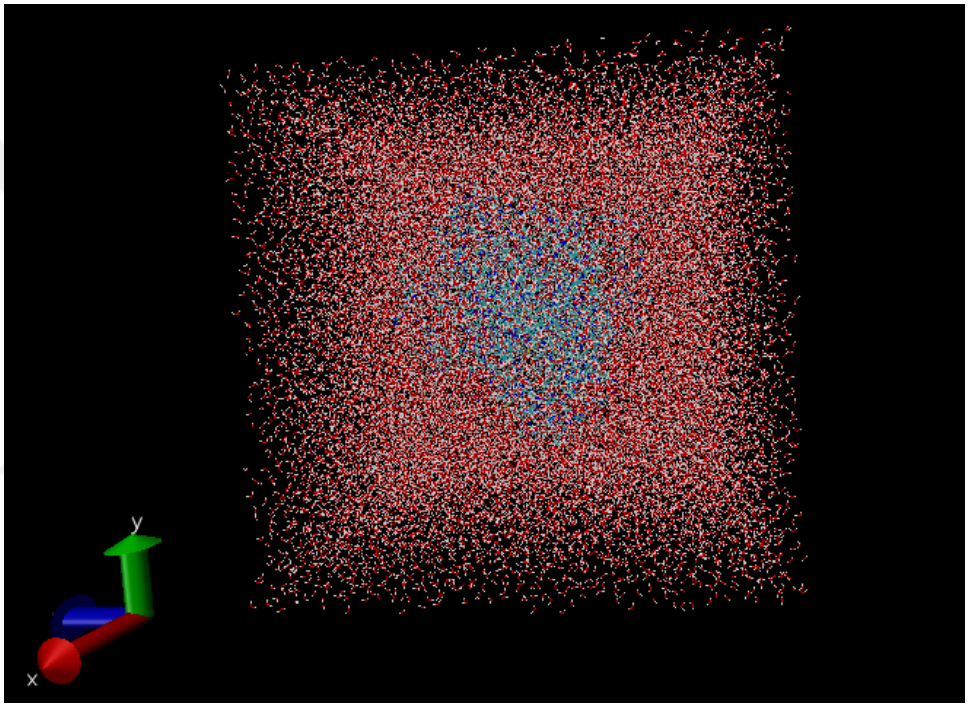

Figure 20: Procaspase-1 (pdb ID: 3E4C (without C285A mutation)-Colchicine Complex and Water Box Representation in VMD

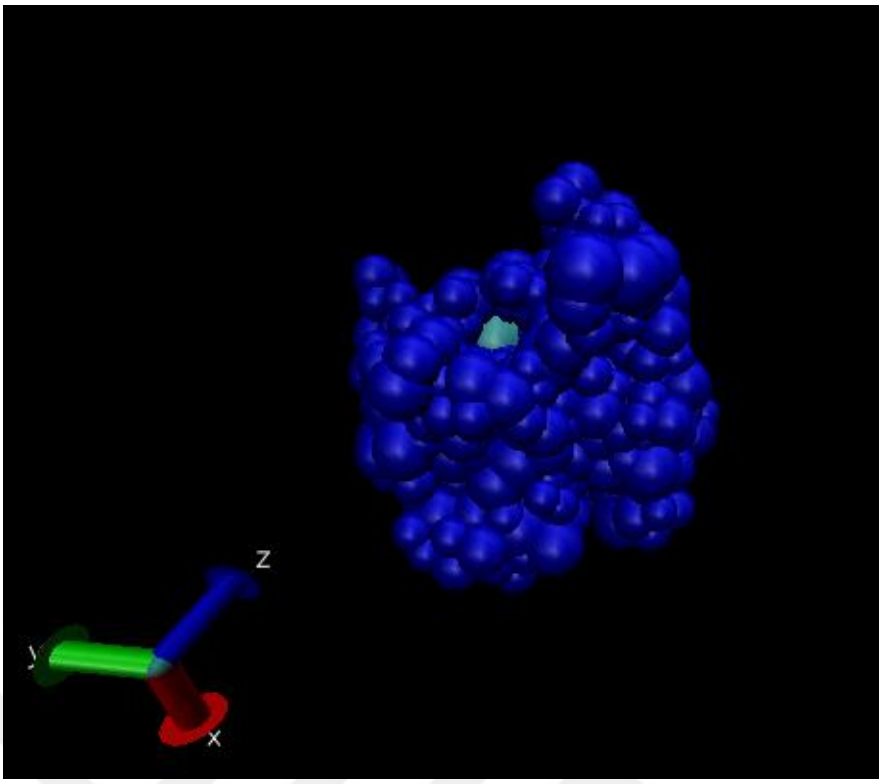

Figure 21: Procaspase-1 (pdb ID: 3E4C (without C285A mutation)-Colchicine Complex in VMD

3.3 Calculation of Fluctuations in Trajectory

Simulation give position vector $R_i(t_k)$ for every carbon alpha atom i at every time t_k.

N_T is the total number of time steps of the trajectory, which is 1000 for each case. First, time average was calculated by using Equation.1.

$$\bar{R}_i = \sum_{t_k} R_i(t_k) / N_T \qquad \text{Equation.1}$$

Then the instantaneous fluctuation $\Delta R_i(t_k)$ of the position vector of i^{th} atom is obtained by using Equation.2.

$$\Delta R_i(t_k) = R_i(t_k) - \bar{R}_i \qquad \text{Equation.2}$$

Root mean squared fluctuations for each atom i is found by Equation.3 which includes dot product.

$$\text{RMSF}=\left\langle \left(\Delta R_i\right)^2 \right\rangle^{0.5} \qquad \text{Equation.3}$$

3.4 B-factor Calculation

B factor is a measure of thermal motion [73]. Crystal structures obtained from Protein Data Bank have experimentally measured b-factors. By using the simulation results and correlated fluctuations in the trajectory b-factors can also be calculated using the Equation.1. $\langle(\Delta R_i)^2\rangle$ denotes the time independent autocorrelation of fluctuations of i^{th} atom, whereas B_i shows the B factor of i^{th} atom.

$$B_i = \frac{8\pi^2}{3}\langle(\Delta R_i)^2\rangle \qquad \text{Equation.4}$$

3.5 Pearson Correlation Coefficient Matrix

$C\left(\Delta R_i, \Delta R_j\right)$ states for Pearson Correlation Coefficient Matrix and each correlation between two atoms were obtained by using Equation.5.

$$C_{ij} = C\left(\Delta R_i, \Delta R_j\right) = \frac{\left\langle \Delta R_i \cdot \Delta R_j \right\rangle}{\left\langle \left(\Delta R_i\right)^2 \right\rangle^{1/2} \left\langle \left(\Delta R_j\right)^2 \right\rangle^{1/2}} = \frac{\sum_{t_k=1}^{N_T} \Delta R_i\left(t_k\right) \cdot \Delta R_j\left(t_k\right)}{\left[\sum_{t_k=1}^{N_T} \left(\Delta R_i{}^2\left(t_k\right)\right)\right]^{1/2} \left[\sum_{t_k=1}^{N_T} \left(\Delta R_j{}^2\left(t_k\right)\right)\right]^{1/2}}$$

Equation.5

Pearson Correlation Coefficient matrix gives a value between -1 and 1 which shows how two atoms are correlated. If two atoms move parallel to each other and positively correlated then Pearson Coefficient function is 1. If they move in opposite directions and negatively correlated, then the Pearson Correlation function is -1. If they are not moving parallel or moving independently, then the result is 0.

3.6 Calculation of the Distance Distributions between Residue Pairs

The distances between two residues were calculated for all time points of the trajectory. These distances were then partitioned into different bins and their normalized distribution was obtained. Normalization was made by making the area under the distribution equal to unity.

Chapter 4

4. RESULTS

4.1 Homology Modelling Results

According to normalized Discrete Optimized Protein energy scores (z-DOPE) obtained by Chimera, poor models have positive z-scores, whereas negative values give better models. This score was calculated in accordance with Carbon alpha RMS errors and Pearson correlation functions of designed models, which were explained in detail in the study by Shen and Sali et Al. [68, 69].

Except for model-5 (A-5 in Table-1), all of the other models in chain A created with software gave the same negative z-score which is -1.58 and either can be used to complete the missing linker region in caspase-1. Model A.1 was chosen for missing region in Chain A. On the other hand, Chain B has more variety of models to be selected. Since Model B.5 is the most negative value, it was chosen for chain B of procaspase-1 enzyme.

Table-1: Chimera Modeller Results

Model	z-DOPE score
A.1	-1.58
A.2	-1.58
A.3	-1.58
A.4	-1.58
A.5	-1.54
B.1	-1.49
B.2	-1.52
B.3	-1.53
B.4	-1.52
B.5	-1.55

4.2 Comparison of Calculated and Experimental B-factors

Figure 22 and Figure 23 shows b-factor change through caspase-1 and procaspase-1 enzymes. B-factor is related to degree of dynamic mobility of an atom [73]. Atoms with low b-factors correspond to well-ordered structures, whereas high b-factors indicate very flexible parts of proteins [74].

The line, which represents simulation results higher than X-ray data for both cases. This may be due to the potential of MD simulations to show the heterogeneity which cannot be observed from X-ray data [75]. In Figure 22 the high black peaks which are in the beginning and at the 404^{th} residue indicate that N-terminal and C-terminals of each heterodimer is very flexible. Since the linker region between two subunits in procaspase-1 was completed afterwards, the experimentally measured b-factor data from pdb does not include any data for that region. This lacking can be seen for two dimers where the b factor for red line is zero. On those regions

simulation results are higher, because the linker region is flexible when compared to other subunits.

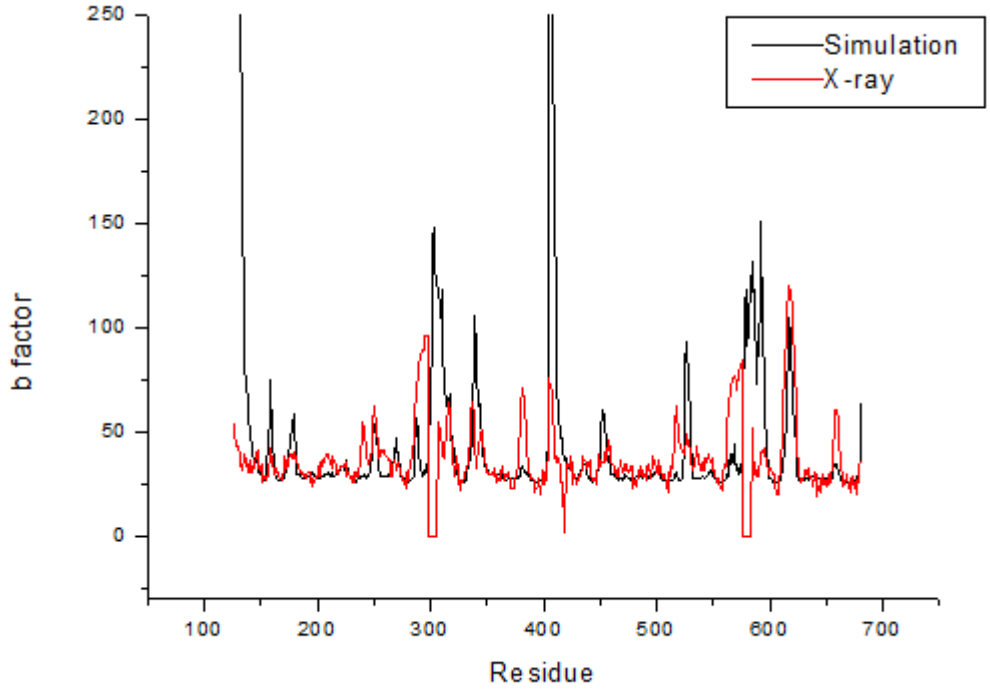

Figure 22: B factor Comparison for Procaspase-1

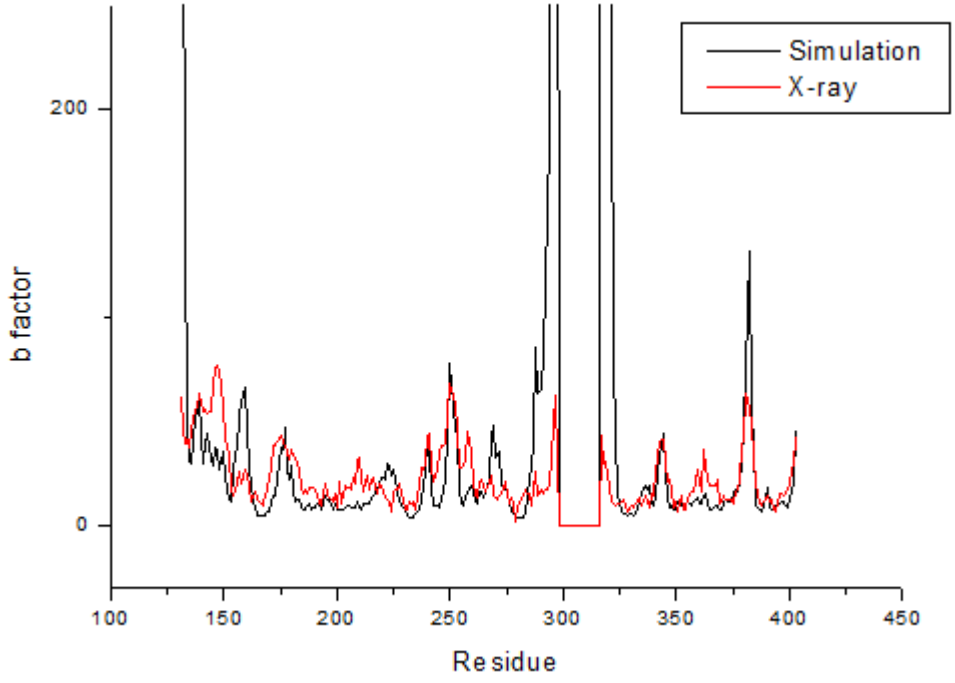

Figure 23: B factor comparison for Caspase-1

In Figure 23 highest red peaks are observed again at the beginning and at the ends of p20 and p10 subunits. Since the residues in the middle of enzyme are more restrained due to their positions, the peak differences are higher compared to the residues having higher level of mobility [76]. Except some differences between two lines, they mostly overlap which shows analogy between simulation and experimental results.

4.3 Pearson Correlation Coefficient Matrix

After the fluctuations through time were combined with Pearson Correlation Coefficient Function calculations, two matrices showing the correlation of each carbon alpha atom in each chain were obtained for procaspase-1 and procaspase-1-colchicine complex. They were illustrated as a grid data on Surfer program (Figure 24, 25). In the figures, green dots show the correlations between 0.5 and 1, while the red dots correspond to correlations from -0.5 to -1. The reason of

demonstrating only some of correlations is to focus on the most positive and the most negative ones.

According to the figures, binding of Colchicine reduces the negative correlations throughout the enzyme, while positive correlations increased.

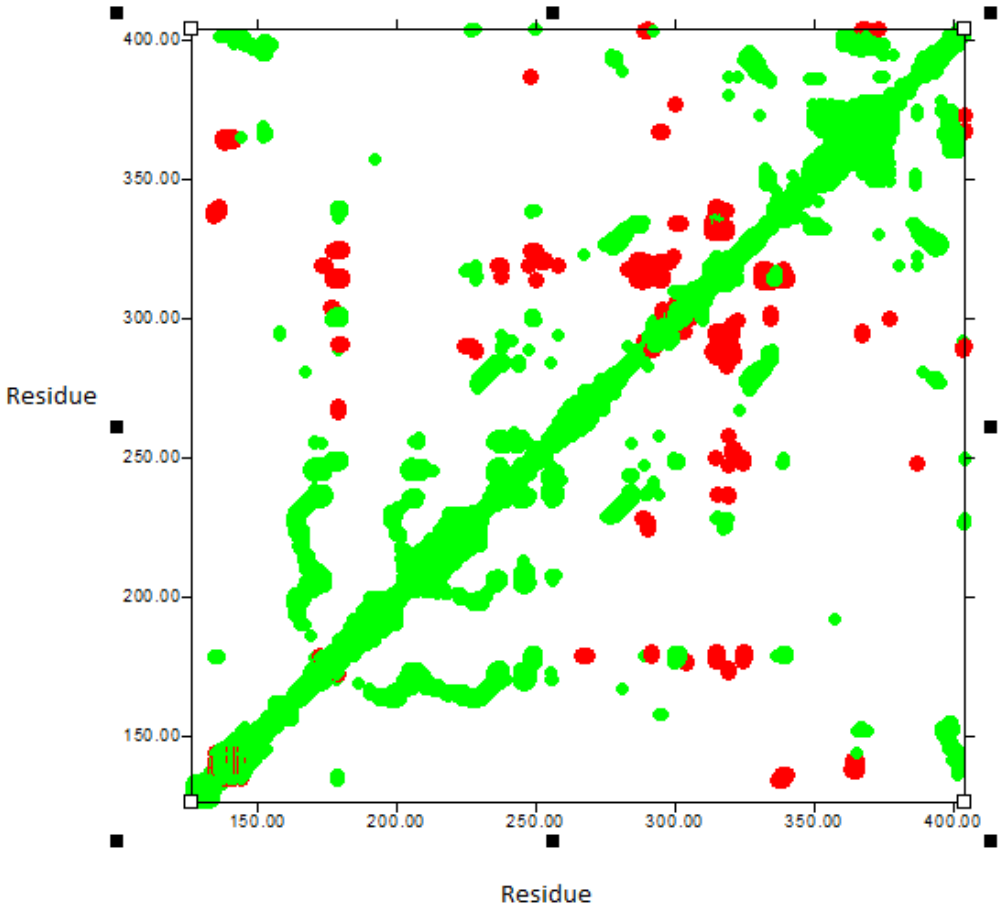

Figure 24: Pearson Coefficient Matrix of Procaspase-1 enzyme (from 126th to 404th residue)

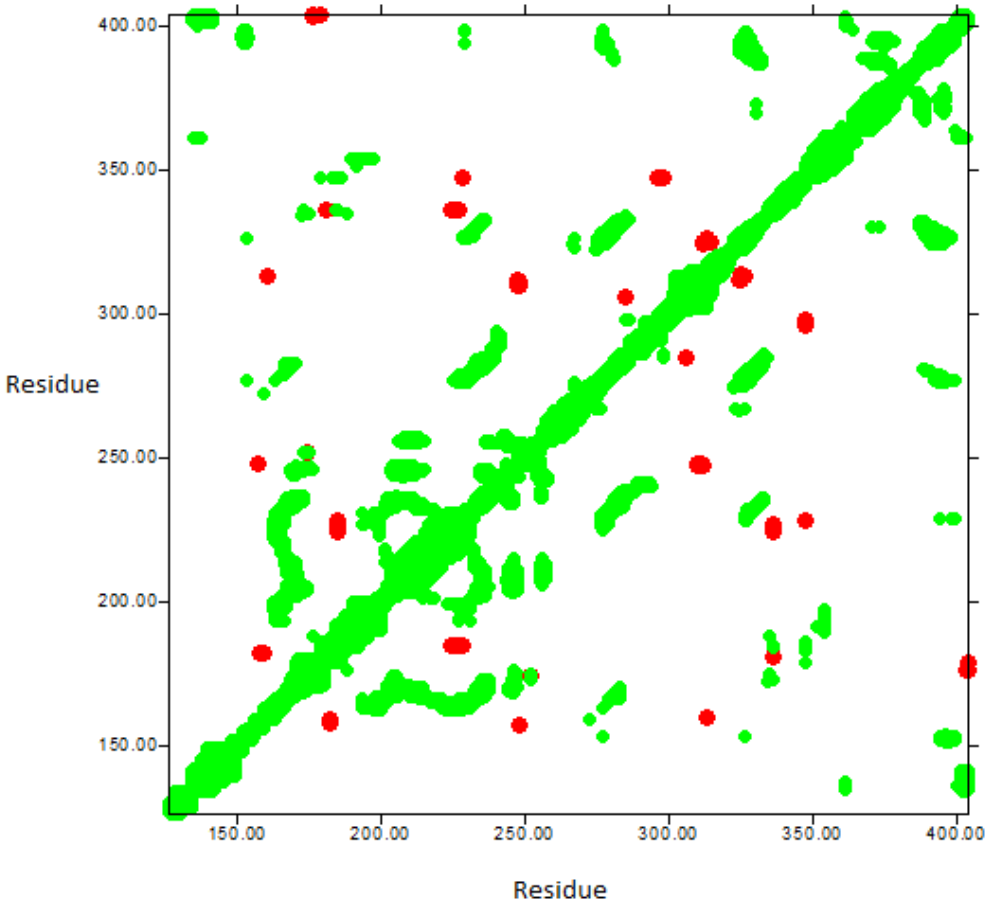

Figure 25: Pearson Coefficient Matrix for Procaspase-1-Colchicine Complex (from 126th to 404th residue)

Chapter 5

5. DISCUSSION

5.1 Distance Changes between Residue Pairs

Allosteric regulation of the caspase-1 enzyme induces a circuit, which forms two conformational states. The aim of this study is to observe how binding of colchicine to the dimer-dimer interface -allosteric site of the enzyme- in caspase-1 expectantly reduces the activation of the enzyme. Therefore, conformational changes in the active site are significant, since binding of a ligand to allosteric site inhibits the active site pocket and inactivates the enzyme (Figure 5).

This section focuses on important residues in the active site region, which are responsible for activation of the enzyme. These residues are Arg179, Thr180, His237, Gln283, Cys285 in p20 subunit; Cys331, Asp336, Arg341 and Arg383 in p10 subunit (Figure 26). They either participate in interactions with the active-site inhibitor molecule or stabilize the ligand molecule in that position and assist in activation of the enzyme. To observe the conformational changes of the enzyme, the distances between these residue pairs for all time steps were calculated.

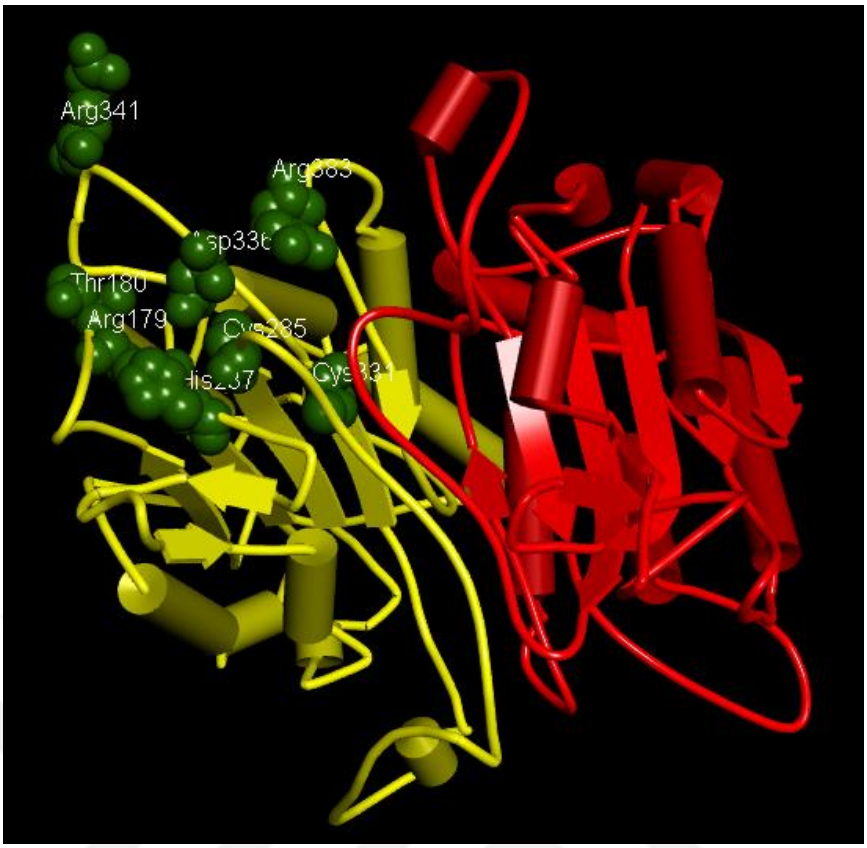

Figure 26: Active Site Region and the Significant Residues in Chain A with CPK Representation.

The residues Cys285 and His237 which are responsible for the catalysis reaction of the enzyme are shown in Figure 27. The normalized distance distribution before and after colchicine is bound can be seen in Figure 28. The figure shows that after ligand is bound, distances between Cys285 and His237 residues increase, which may affect the activation mechanism. The closer they are to each other, the more possible they form a hydrogen-bond network.

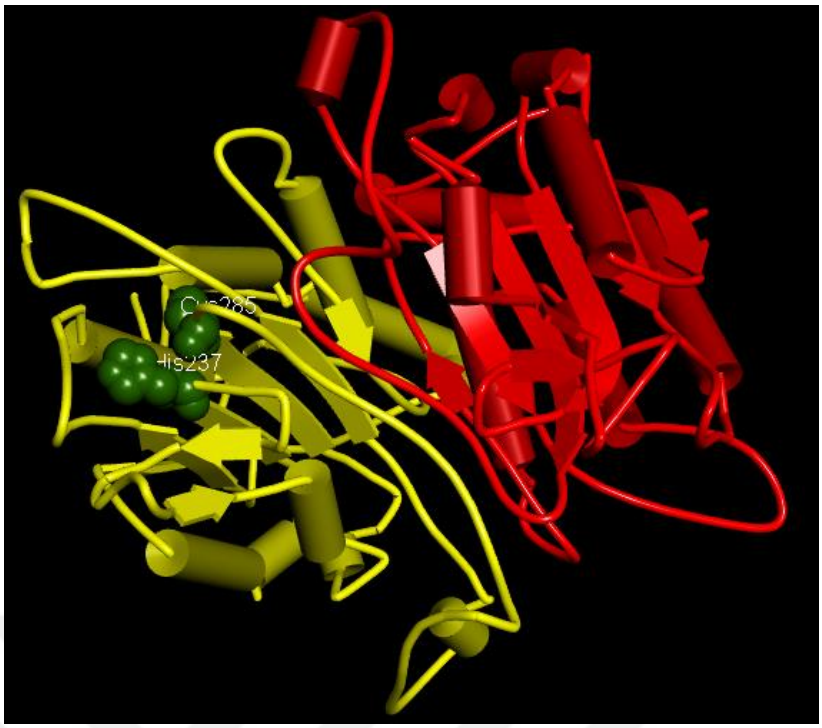

Figure 27: CPK representation of Cys285 and Cys237 residues

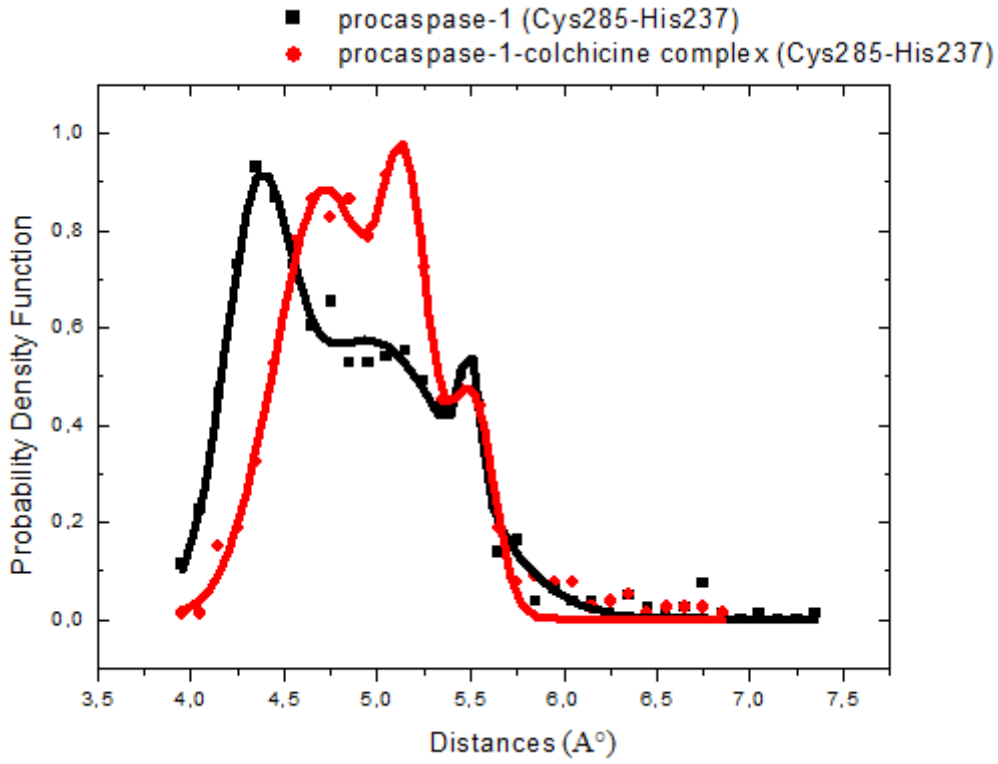

Figure 28: Probability Density Function of Distances between Cys285 and His237 residue pair

The other two important residue pairs are Arg179-Arg341 and Thr180-Arg341 which are shown together in Figure 29, and their normalized distance distributions are shown in Figures 30 and 31, respectively.

As indicated in the Literature Review section, Arg179 and Arg341 should form hydrogen bonds with the substrate in order to activate the enzyme, and Arg341 should interact with Thr180 in order to stabilize its position. Therefore, it is important for them to be adjacent to each other for activation. From the Figure 30 and 31, it can be seen that binding of colchicine to the dimer-dimer interface in caspase-1 increases the distance between these important residues which may affect the stability of L1 and L3 loops, thereby prohibiting activation.

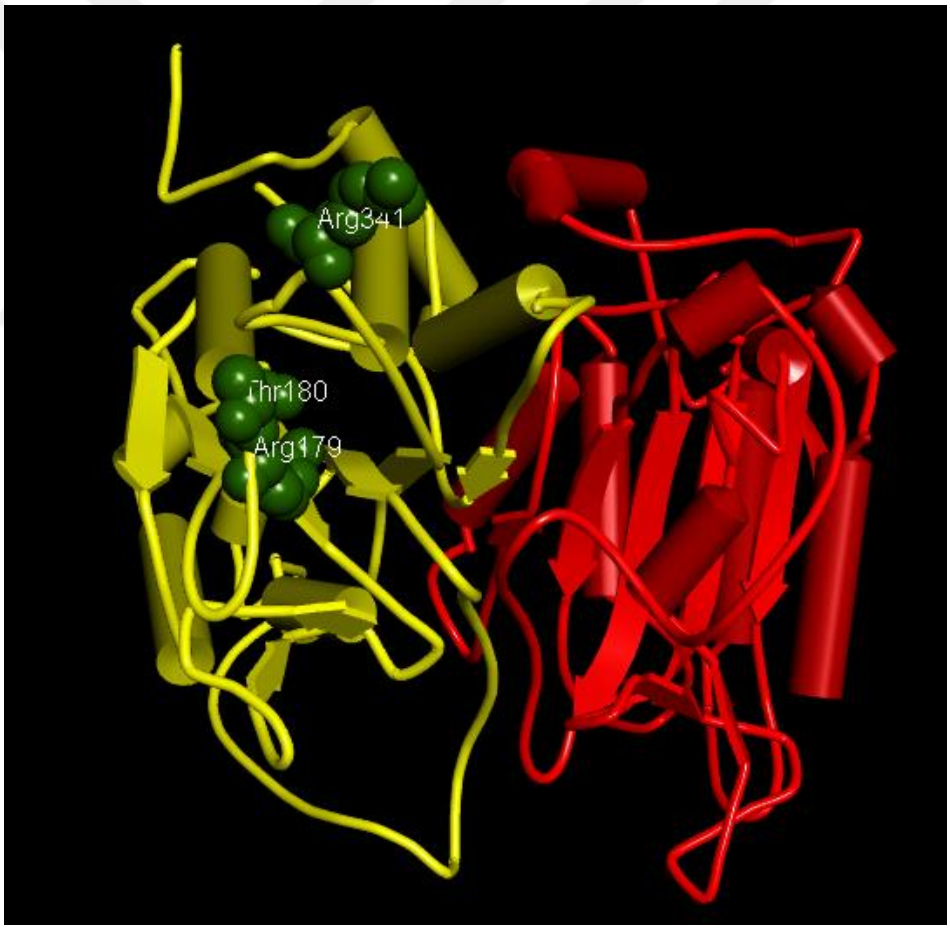

Figure 29: CPK representation of Arg179, Thr180 and Arg341 residues

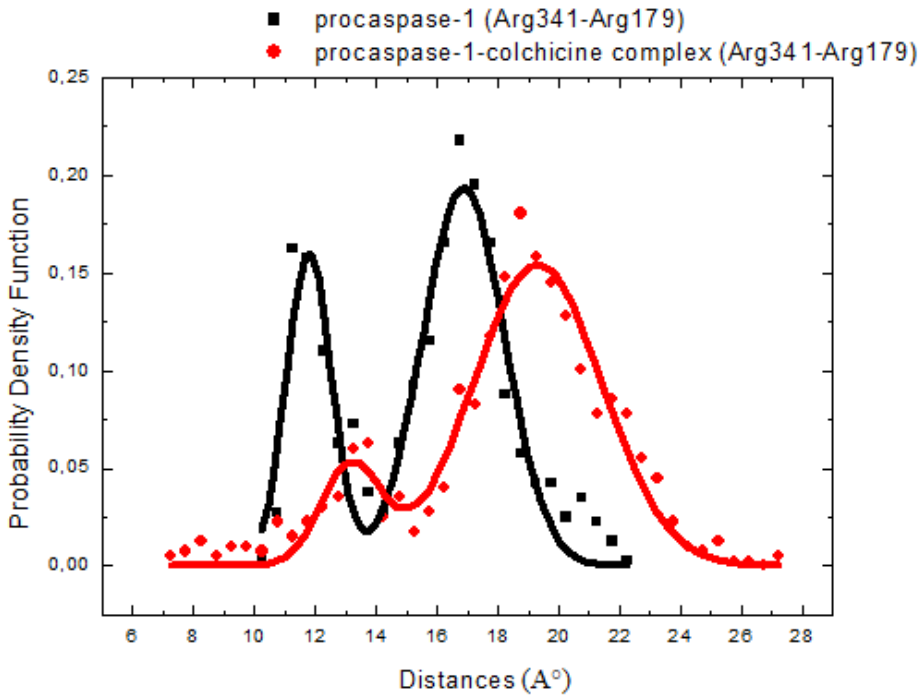

Figure 30: Probability Density Function of Distances between Arg341 and Arg179 residue pair

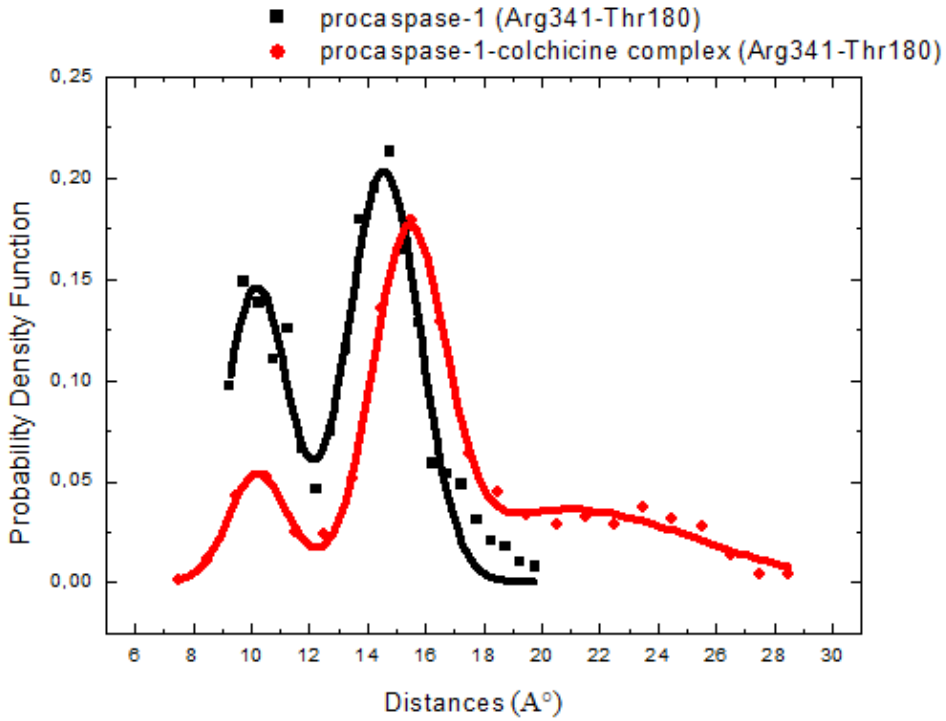

Figure 31: Probability Density Function of Distances between Arg341 and Thr180 residue pair

Figure 32 demonstrates Asp336 and Arg383 which make salt bridges in the active binding pocket. According to the studies which were explained in detail in Literature Review section, removal of this salt bridge can induce the activation of the enzyme. According to our analysis which is shown in Figure 33 after the binding of colchicine, the distance between pair decreases as expected. Although probability distribution between the pair in procaspase-1-colchicine case varies in a long range, the distances between them mostly low as it can be seen from the highest peak when compared to other probability distributions. Also when the trajectory was observed in detail, it was seen that the distance between Asp336 and 383 decreases during time after binding.

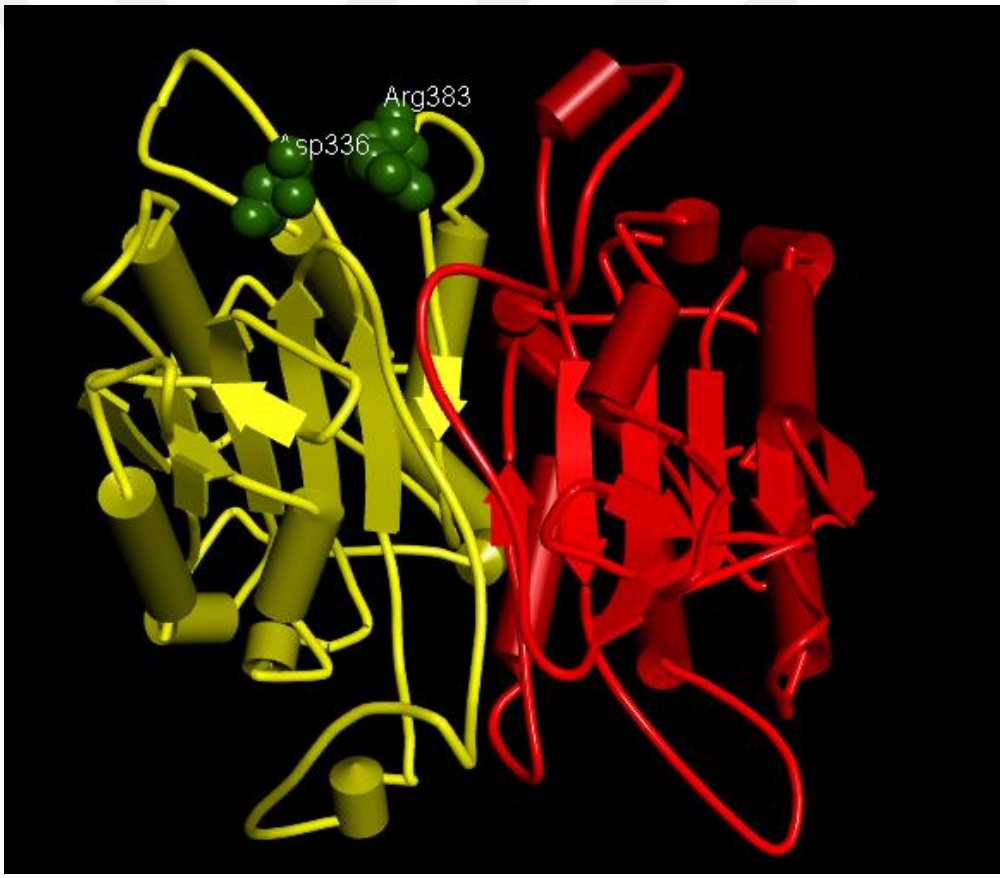

Figure 32: CPK representation of Asp336 and Arg383 residues

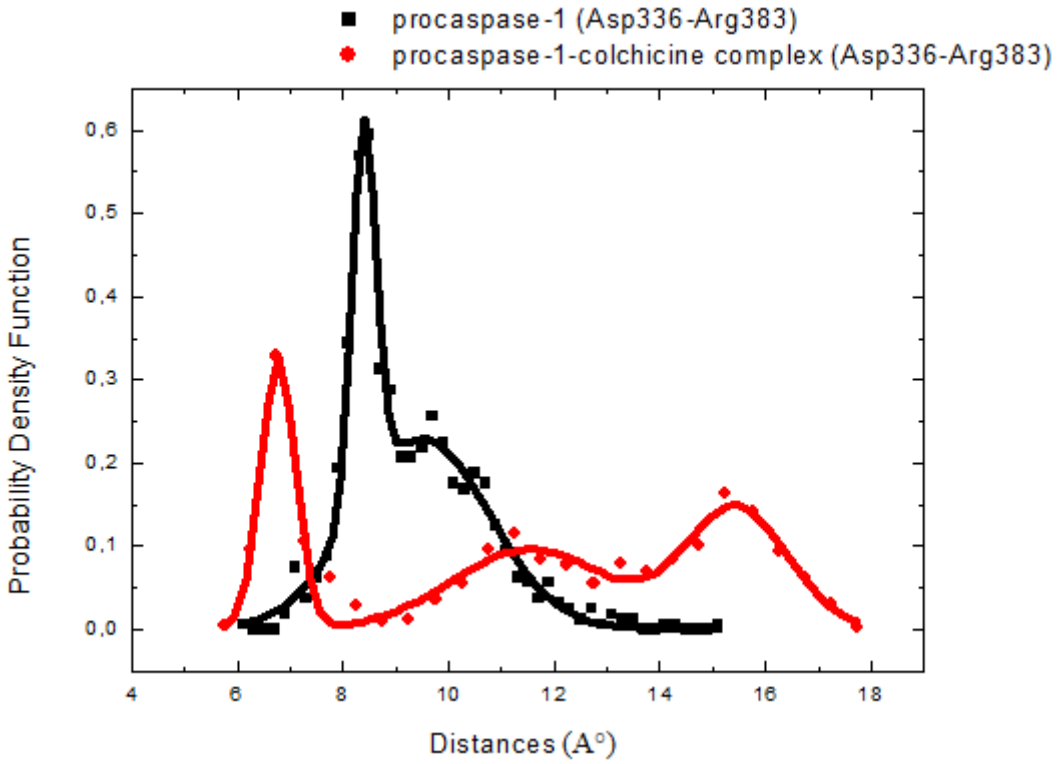

Figure 33: Probability Density Function of Distances between Asp336 and Arg383 residue pair

After significant interactions in the active site were examined, different combinations of these residues were also investigated to see if there is any large conformational change in active site region after colchicine binding.

Figure 34 was taken from 1ICE pdb structure which shows active caspase-1 enzyme complex with a tetra-peptide inhibitor. The illustrated residues are Arg179, Asp336, Arg383 and Arg341 in Figure 34 and 35. The distance between Asp336 and Arg383 in Figure 34, which represents the caspase-1 active enzyme structure, is bigger when compared to inactive enzyme structure in Figure 35. As expected, the breakage of salt bridge may be one of the reasons of active site formation. Since these four residues surround the active site substrate, it is important to see how they affect the cleft by calculating the distance change for all time steps for each residue pair.

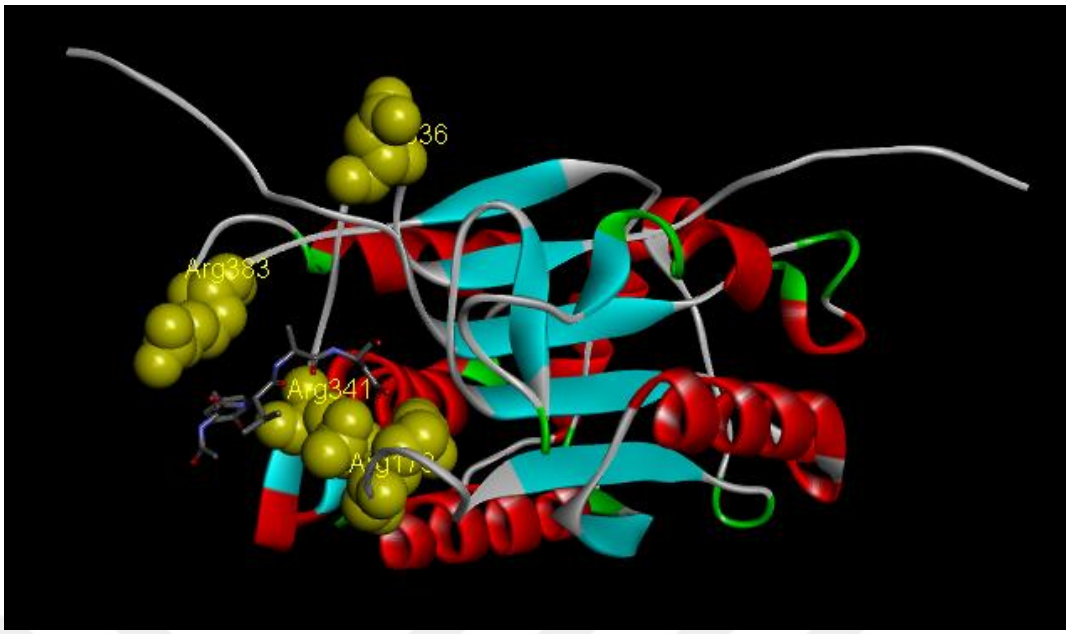

Figure 34: Representation of Some significant residues in active caspase-1 (pdb Id: 1ICE) with a tetrapeptide inhibitor

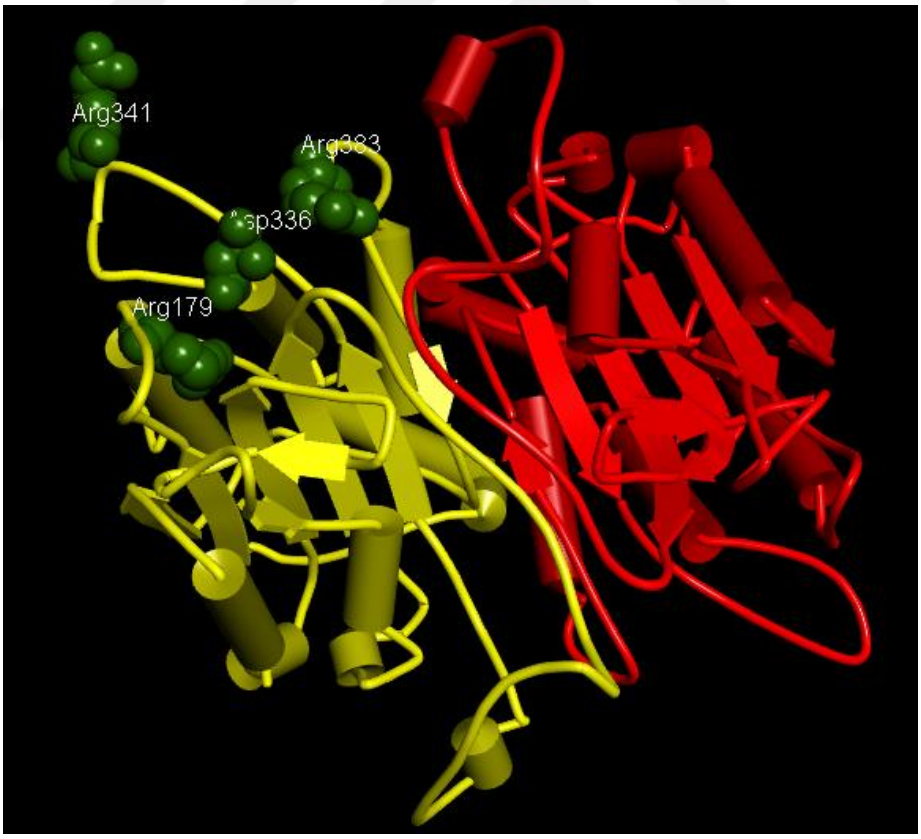

Figure 35: CPK representation of Arg179, Asp336, Arg341 and Arg383 residues (This conformation is from the last one-tenth of the time trajectory.)

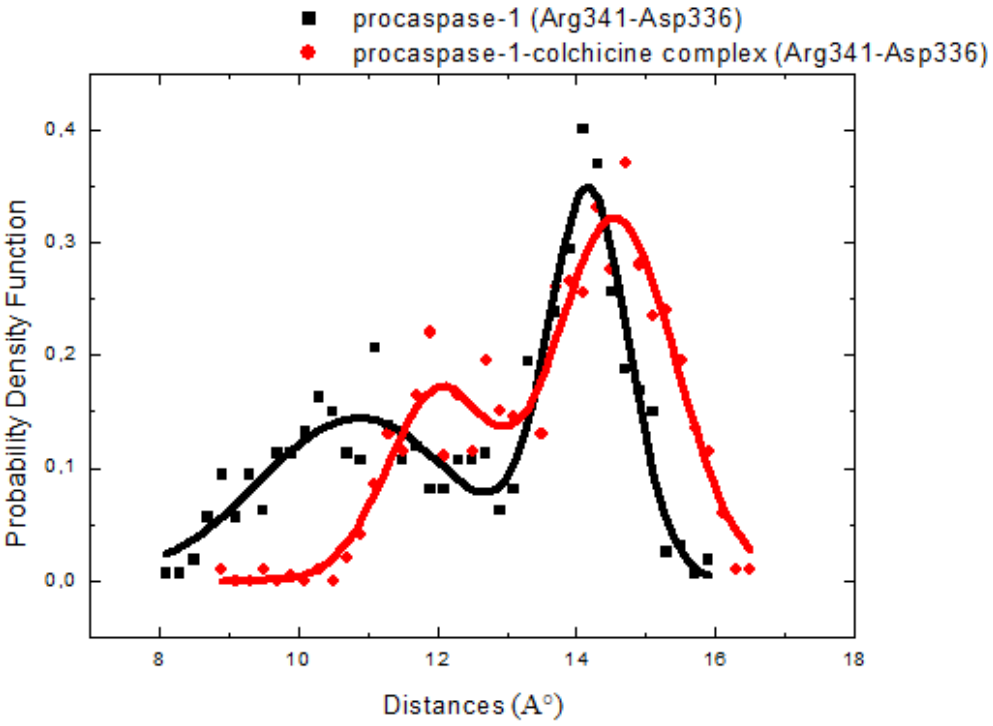

Figure 36: Probability Density Function of Distances between Asp336 and Arg341 residue pair

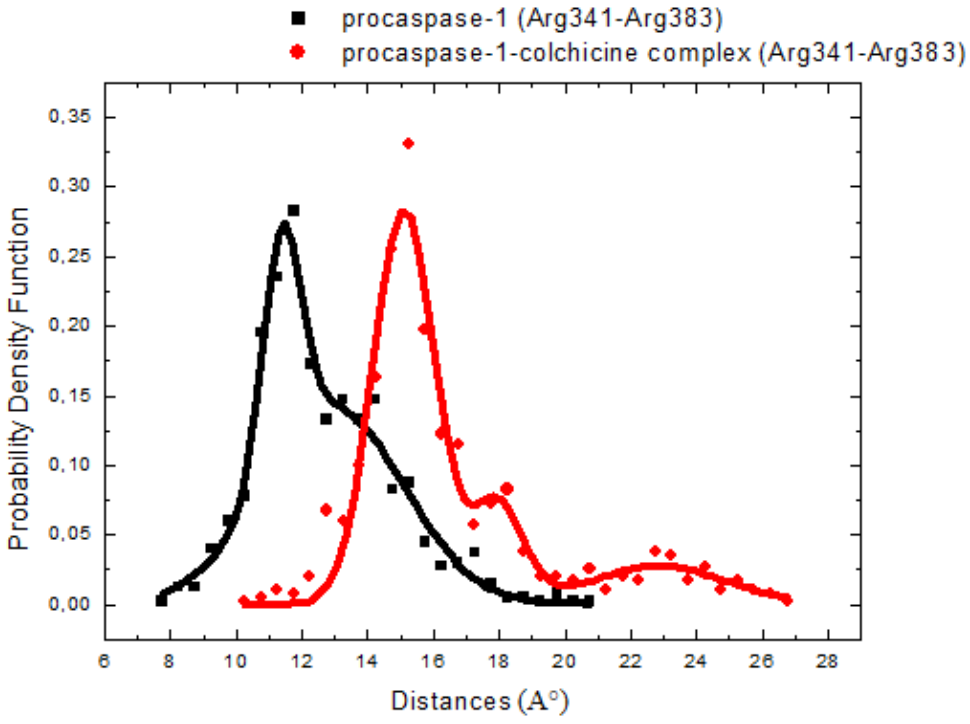

Figure 37: Probability Density Function of Distances between Arg341 and Arg383 residue pair

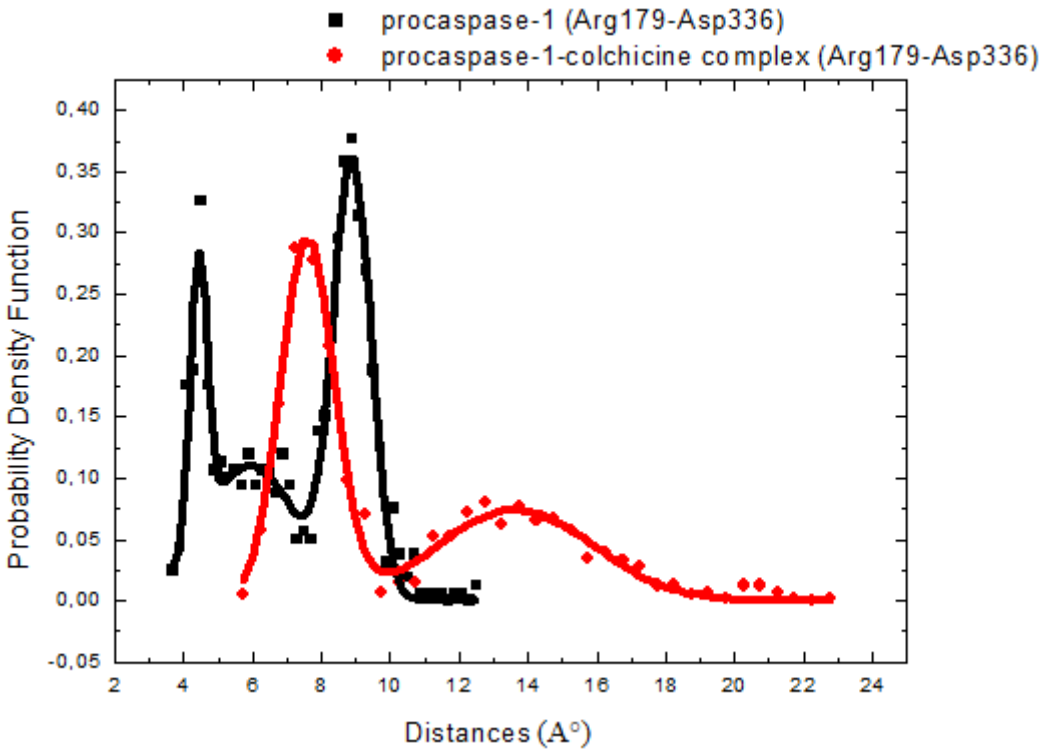

Figure 38: Probability Density Function of Distances between Arg179 and Asp336 residue pair

Figure 9 (in Literature Review section) demonstrates active site pocket in accordance with loops. Considering that phenomenon the distances between key residues in active site pocket was examined. First when the conformational changes before and after colchicine is bound to enzyme is compared to each other, between each residue pair there is a considering amount of shift throughout the trajectory. As can be seen from the Figure 36, the distance change between the residues in L3 loop which are Asp336 and Arg341 is not remarkable. However there are apparent increases between Arg341-Arg179 (Figure 30) and Arg341-383 (Figure 37). This may show that Arg341 with L3 loop rotate in opposite direction by holding the distance constant with Asp336, but opposing from Arg179 (L1 loop) and Arg383 (L4 loop). So this change may break the active site cleft and affect whole protein dynamics.

The interaction between Arg179-Asp336 and Arg383 is another important case which needs to be taken into account. Two different salt bridges –Arg179/Asp336 and Asp336/Arg383- are formed before and after the colchicine is bound. According to the studies by Amor, Yaliraki et al.

it is known that the presence of the Asp336-Arg383 salt bridge is important for the enzyme to remain inactive. When the MD trajectory is observed in detail, it was seen that the distances between residues Arg383 and Asp336 decreases with time. On the other hand, the opposite is true for the other salt bridge (Arg179-Asp336). For this interaction, distances between these residues are first small and then start to increase which ends in breakage of this salt bridge. From these observations, when the middle-positioned residue Asp336 comes closer and makes a salt bridge with one of these residues, the other salt bridge may not form. Also Figure 38 and Figure 33 indicate that after the colchicine is bound (represented with red line); the distances between salt bridges vary from approximately 5 to 20 Angstroms. This triad interaction has a strong effect on protein activation. In support of the studies by Amor, Yaliraki et al., Arg383-Asp336 salt bridge was observed in our trajectory which may be an interaction that inhibits activation.

5.2 Pearson Correlation Coefficient Function

Pearson Correlation function shows the dependence of the motions of two atoms as mentioned in the previous sections (Figure 24 and 25). From the Pearson correlation matrix representations in Results section, it was observed that the negative correlations decreased and positive correlations increased after colchicine was bound to enzyme. This may be interpreted as binding of colchicine in dimer interface may change dynamics of the enzyme. Hence, this change may inhibit the activation of protein.

In Figures 39 and 40 each residue which is shown with red has a high negative correlation with each blue colored-residue. In the Figures only the highest negative correlations were shown which are 13 in procaspase-1 and 6 in procaspase-1-colchicine complex (Figure 39 and 40). The arrows indicate predicted direction of motion according to these simulations. Since procaspase-1 enzyme has more negative correlations when compared to procaspase-1-colchicine complex, it can be said that the prolongation motion in procaspase-1-colchicine complex may be lowered.

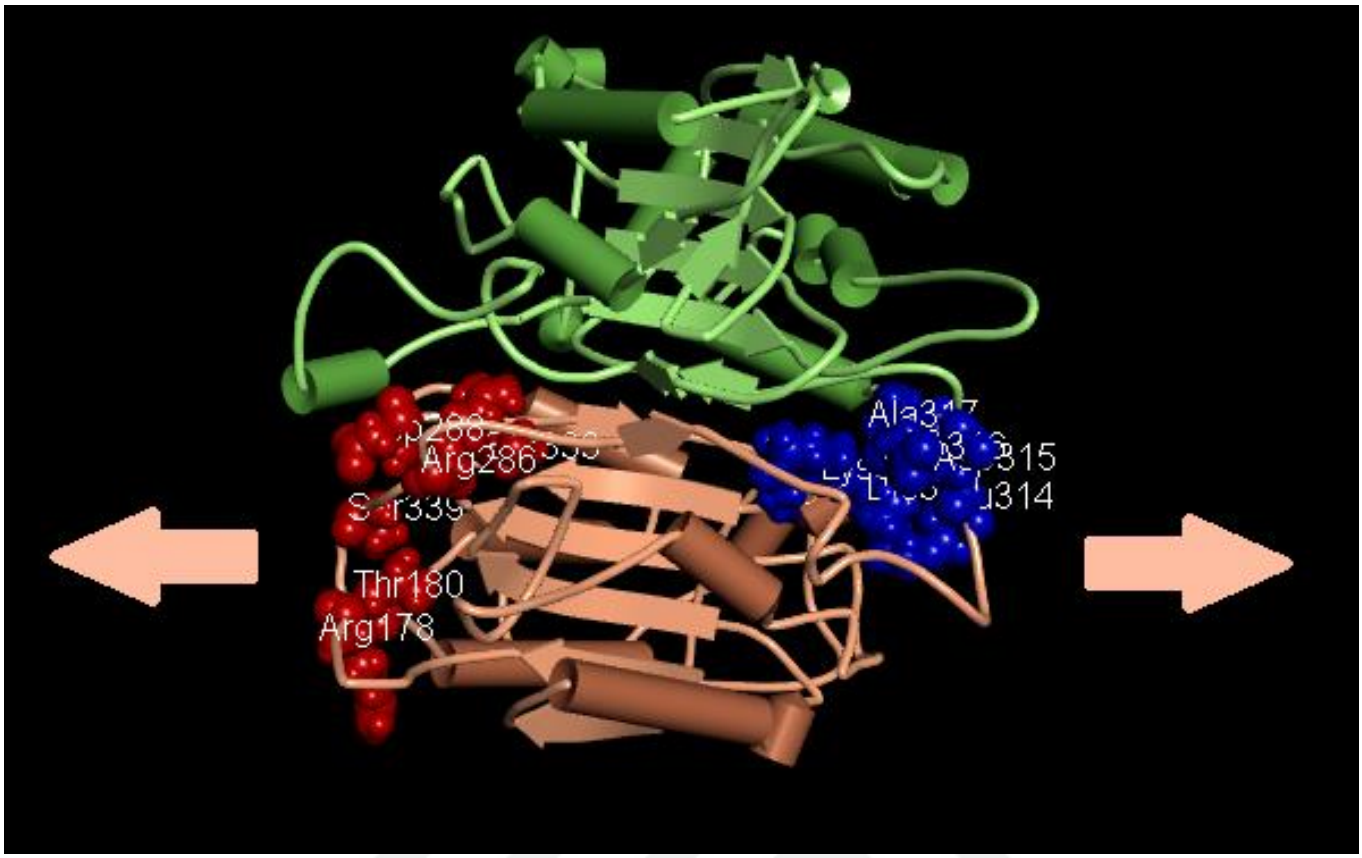

Figure 39: Demonstration of Negative Correlations in A chain of Procaspase-1.

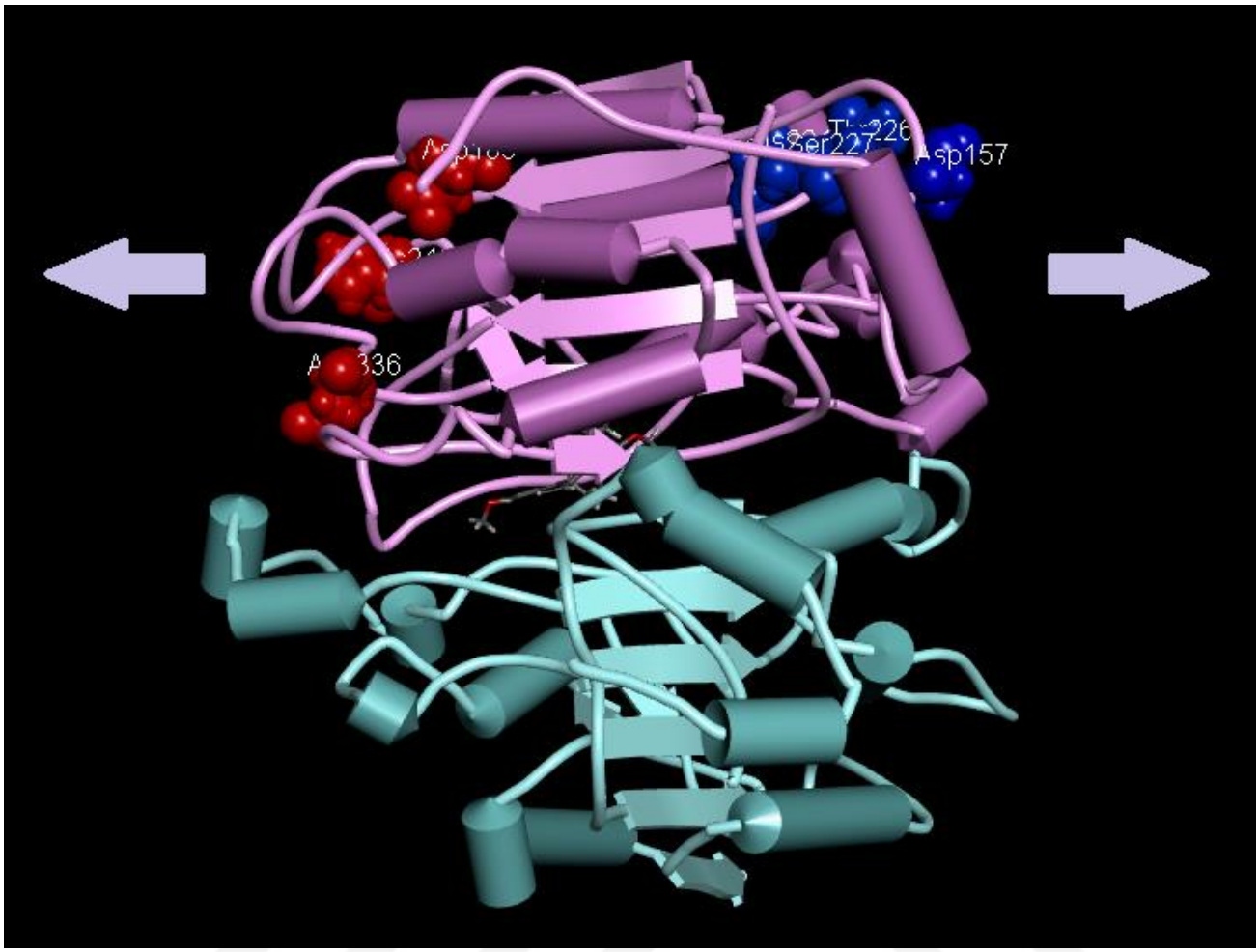

Figure 40: Demonstration of Negative Correlations in A chain of Procaspase-1-colchicine Complex.

5.3 Distance Changes in Cleavage Site

As mentioned in previous sections, caspase-1 enzyme is activated through auto-proteolysis. Cys285 and His237 residues in one dimer forms a catalytic region with Asp297 and Asp316 residues in other dimer, therefore it cleaves the linker region between large and small subunits. In this section, we will try to examine whether binding of colchicine affects these cleavage reactions or not by comparing the distance changes in each residue pair.

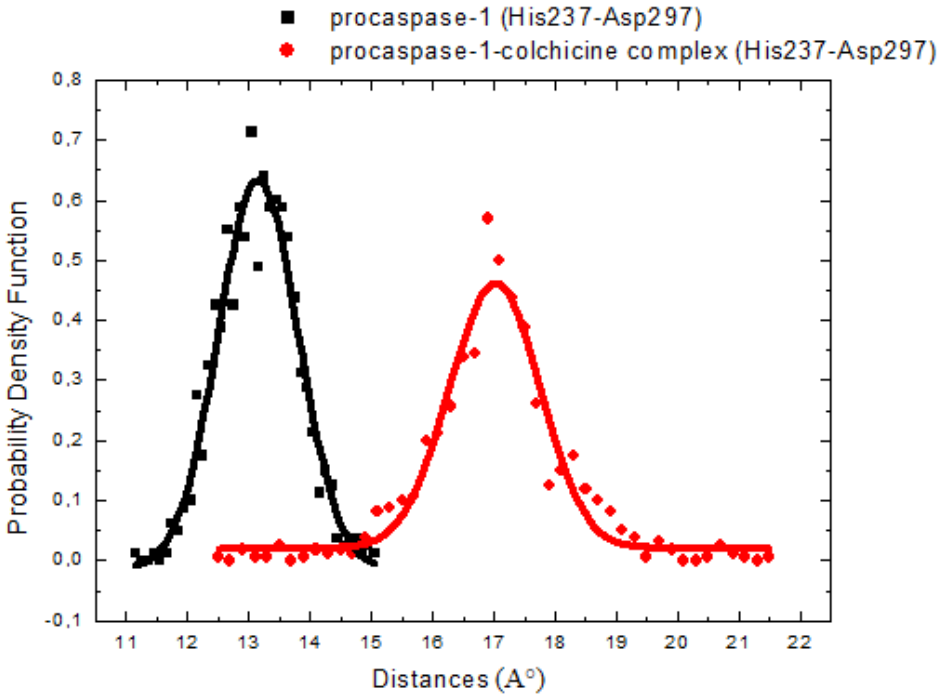

Figure 41: Probability Density Function of Distances between His237 and Asp297 residue pair

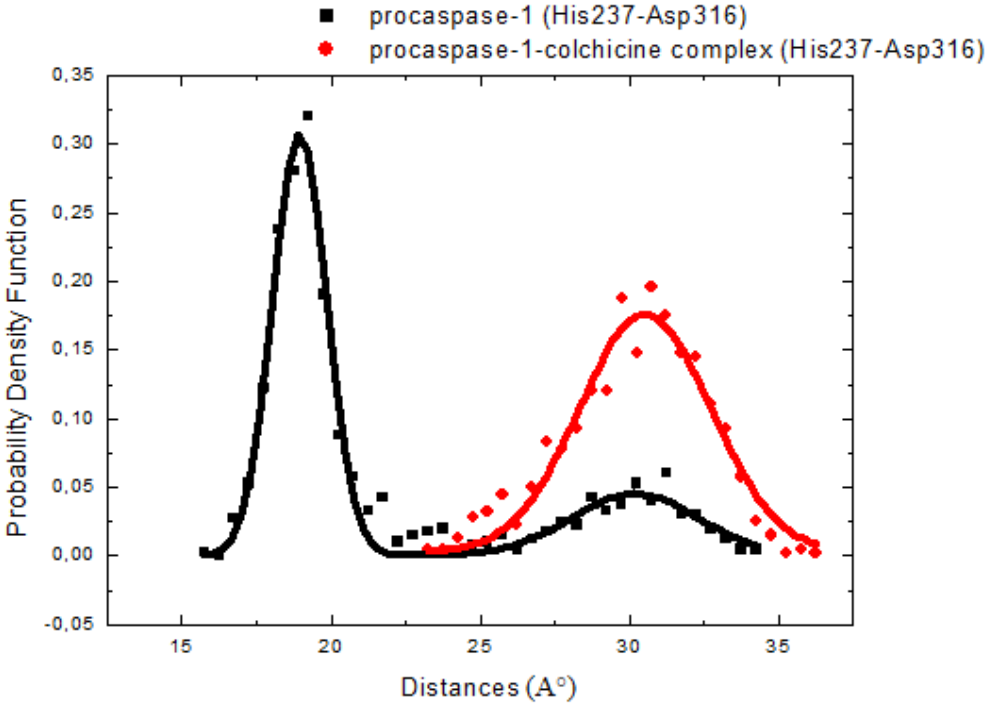

Figure 42: Probability Density Function of Distances between His237 and Asp316 residue pair

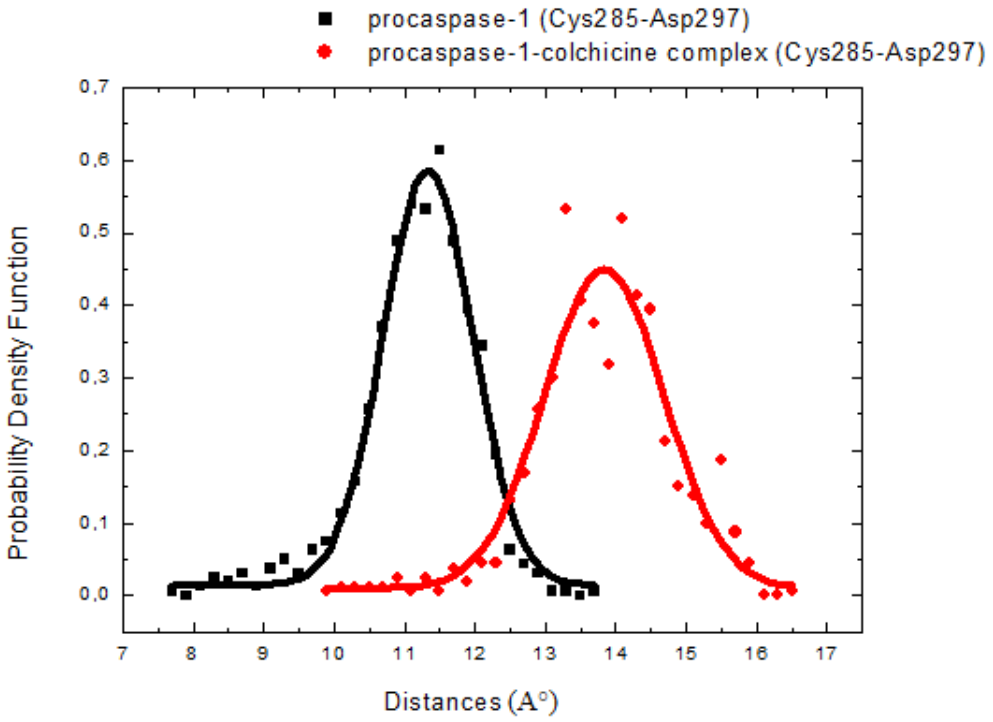

Figure 43: Probability Density Function of Distances between Cys285 and Asp297 residue pair

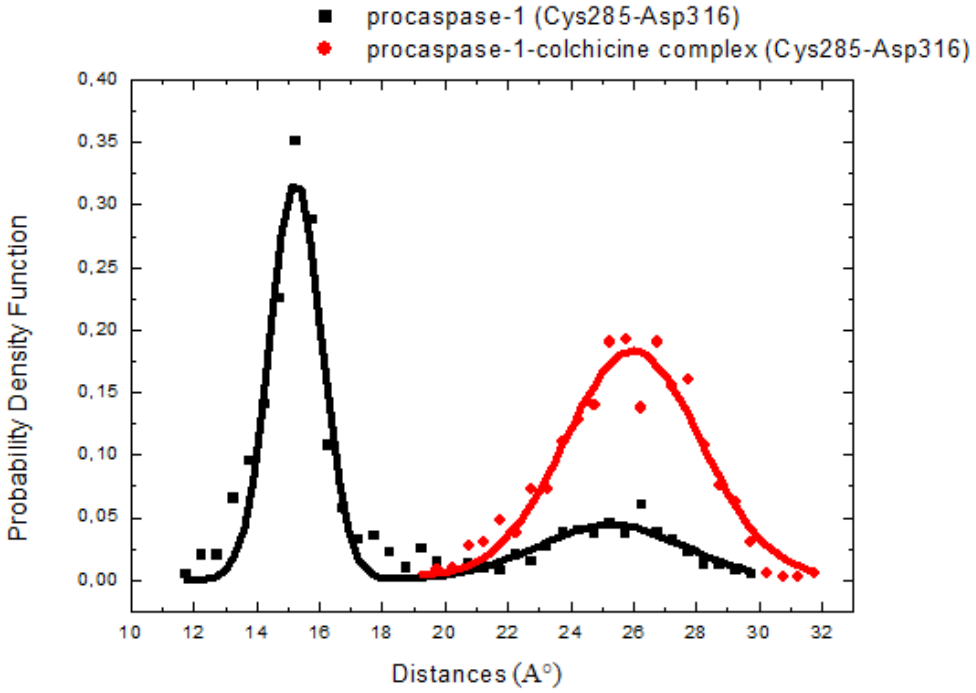

Figure 44: Probability Density Function of Distances between Cys285 and Asp316 residue pair

According to the structural and kinetic analysis by Elliott and Rouge et al. it was observed that first proteolytic reaction takes place at Asp297 residue which is in N-terminal of linker region between subunits. After it is cleaved, second cleavage occurs at Asp316. In Figure 41 and 43 it can be seen that binding of colchicine increases the distance between the catalytic residues and Asp297, therefore reduces the probability of cleavage reaction on Asp297 residue. [7]

In Figure 42 and 44, the black lines have two peaks. In the beginning of the trajectory His237 and Cys285 are far from Asp316, but during the 600-ns period of time the distances between them decreases. This shows that before the colchicine binding the linker region between Asp297 and Asp316 is able to be flexible to a great extent. After colchicine is bound, Asp316 cannot reduce the distance between active site residues to which it is cleaved. Also this reduce may show that a network of allosteric regulation affects Asp316.

Chapter 6

6. CONCLUSION

In this computational study, the aim was to observe structural changes in active site after colchicine drug is bound to dimer-dimer interface which also supports that the enzyme is allosterically regulated. Pearson Correlation Coefficient matrix was calculated for the procaspase-1 and procaspase-1+colchicine complex, and correlation changes were observed after colchicine is bound. Longwise negative correlations decreased and positive correlations increased throughout the enzyme. Also the patterns of most positive correlations changed appreciable which is also a promising sign of responsive allosteric interactions.

Residues which are responsible for activation and proteolytic cleavage were observed in detail. For the proteolytic cleavage part of the observations, after colchicine binding, expected coordinates required for the cleavage reactions cannot be maintained. Asp316 and Asp297 residues which confine the linker region between subunits, stays distant from active site pocket. The distances between residues which are shown in Figures are between carbon alpha atoms of each residue. For the future analysis, the exact distance between interacting atoms may be combined for the method of this study.

For the active site part of the calculations, distances between each residue pair were observed. According to the results, for most cases, binding of colchicine increase the distances when decreasing is required for activation. Ultimately the active site pocket sustains conformational changes induced by colchicine binding that may affect the whole dynamics of the protein.

For further analysis, each residue in the active site pocket is mutated and molecular dynamics simulations may be performed for each different mutation. By changing each of them as a parameter, effect of each mutated residue may be monitored through this allosteric inhibition. Also other drugs may be tested in order to investigate the accuracy of method and studies.

7. BIBLIOGRAPHY

1. Romanowski, M.J., et al., *Article: Crystal Structures of a Ligand-free and Malonate-Bound Human Caspase-1. Implications for the Mechanism of Substrate Binding.* Structure, 2004. **12**: p. 1361-1371.
2. Franchi, L., et al., *The inflammasome: a caspase-1-activation platform that regulates immune responses and disease pathogenesis.* Nat Immunol, 2009. **10**(3): p. 241-247.
3. Hauske, P., et al., *Allosteric Regulation of Proteases*.
4. Alnemri, E.S., et al., *Human ICE/CED-3 Protease Nomenclature.* Cell, 1996. **87**(2): p. 171.
5. Susin, S.A., N. Zamzami, and G. Kroemer, *Mitochondria as regulators of apoptosis: doubt no more*.
6. Donepudi, M. and M.G. Grütter, *Structure and zymogen activation of caspases.* Biophysical Chemistry, 2002. **101**: p. 145-153.
7. Elliott, J.M., et al., *Crystal Structure of Procaspase-1 Zymogen Domain Reveals Insight into Inflammatory Caspase Autoactivation.* JOURNAL OF BIOLOGICAL CHEMISTRY, 2009. **284**(10): p. 6546-6553.
8. Boatright, K.M. and G.S. Salvesen, *Mechanisms of caspase activation.* Current Opinion in Cell Biology, 2003. **15**: p. 725-731.
9. Stennicke, H.R. and G.S. Salvesen, *Caspases - controlling intracellular signals by protease zymogen activation*.
10. Nicholson, D.W. and N.A. Thornberry, *Caspases: killer proteases.* Trends in Biochemical Sciences, 1997(8): p. 299.
11. Martinon, F. and J. Tschopp, *Inflammatory caspases and inflammasomes: master switches of inflammation*.
12. Shi, Y., *Minireview: Caspase Activation. Revisiting the Induced Proximity Model.* Cell, 2004. **117**: p. 855-858.
13. Shi, Y., *Review: Mechanisms of Caspase Activation and Inhibition during Apoptosis.* Molecular Cell, 2002. **9**: p. 459-470.
14. Pop, C. and G.S. Salvesen, *Human Caspases: Activation, Specificity, and Regulation*.
15. Siehs, C., et al., *Discrete simulation of regulatory homo- and heterodimerization in the apoptosis effector phase.* BIOINFORMATICS, 2002. **18**(1): p. 67-76.
16. Green, D. and G. Kroemer, *The central executioners of apoptosis: caspases or mitochondria?* Trends In Cell Biology, 1998. **8**(7): p. 267-271.

17. Fesik, S.W., *Insights into Programmed Cell Death through Structural Biology.* Cell, 2000. **103**(2): p. 273-282.
18. Fuentes-Prior, P. and G.S. Salvesen, *The protein structures that shape caspase activity, specificity, activation and inhibition*.
19. Martinon, F., K. Burns, and J. Tschopp, *The inflammasome: A molecular platform triggering activation of inflammatory caspases and processing of proIL-beta*.
20. Chowdhury, I., B. Tharakan, and G.K. Bhat, *Review: Caspases — An update.* Comparative Biochemistry and Physiology, Part B, 2008. **151**: p. 10-27.
21. Yu, H.B. and B.B. Finlay, *Review: The Caspase-1 Inflammasome: A Pilot of Innate Immune Responses.* Cell Host & Microbe, 2008. **4**: p. 198-208.
22. Guy, S.S. and M.D. Vishva, *Caspase Activation: The Induced-Proximity Model*. 1999, National Academy of Sciences of the United States of America. p. 10964.
23. Chae, J.J., I. Aksentijevich, and D.L. Kastner, *Advances in the understanding of familial Mediterranean fever and possibilities for targeted therapy.* British Journal Of Hematology, 2009. **146**(5): p. 467-478.
24. Martinon, F., A. Mayor, and J. Tschopp, *The Inflammasomes: Guardians of the Body.* Annual Review of Immunology, 2009: p. 229.
25. Lu, A., et al., *Unified Polymerization Mechanism for the Assembly of ASC-Dependent Inflammasomes.* Cell. **156**(6): p. 1193-1206.
26. Simon, A. and J.W.M. van der Meer, *Pathogenesis of familial periodic fever syndromes or hereditary autoinflammatory syndromes*.
27. Lachmann, H.J., *Clinical Immunology Review Series: An approach to the patient with a periodic fever syndrome.* Clinical and Experimental Immunology, 2011. **165**(3): p. 301-309.
28. Onen, F., *Familial Mediterranean fever.* Rheumatology International, 2006(6): p. 489.
29. Akar, S., et al., *Familial Mediterranean fever: risk factors, causes of death, and prognosis in the Colchicine era*. 2012, Lippincott Williams & Wilkins, WK Health. p. 131.
30. Cush, J.J., *Autoinflammatory Syndromes.* Dermatologic clinics, 2013. **31**(3): p. 471-480.
31. Lovett, D.H. and A. Larsen, *Cell cycle-dependent interleukin 1 gene expression by cultured glomerular mesangial cells.* The Journal Of Clinical Investigation, 1988. **82**(1): p. 115-122.

32. Black, R.A., et al., *Generation of biologically active interleukin-1β by proteolytic cleavage of the inactive precursor*. Journal of Biological Chemistry, 1988. **263**(19): p. 9437-9442.
33. Kostura, M.J., et al., *Identification of a Monocyte Specific Pre-Interleukin 1β Convertase Activity*. 1989, National Academy of Sciences of the United States of America. p. 5227.
34. Tschopp, J., F. Martinon, and K. Burns, *NALPs: a novel protein family involved in inflammation.* Nature Reviews Molecular Cell Biology, 2003. **4**(2): p. 95.
35. Wilson, K.P., et al., *Structure and mechanism of interleukin-1 beta converting enzyme.* Nature, 1994. **370**(6487): p. 270-275.
36. Schönbeck, U., et al., *Human vascular smooth muscle cells express interleukin-1β-converting enzyme (ICE), but inhibit processing of the interleukin-1β precursor by ICE*. Journal of Experimental Medicine, 1997. **185**(7): p. 1287-1294.
37. Cerretti, D.P., et al., *Molecular Cloning of the Interleukin- 1β Converting Enzyme*. 1992, American Society for the Advancement of Science. p. 97.
38. Swaan, P.W., et al., *Sequential processing of human proIL-1β by caspase-1 and subsequent folding determined by a combined in vitro and in silico approach.* Pharmaceutical Research, 2001. **18**(8): p. 1083-1090.
39. Fink, S.L. and B.T. Cookson, *Apoptosis, Pyroptosis, and Necrosis: Mechanistic Description of Dead and Dying Eukaryotic Cells.* Infection and Immunity, 2005. **73**(4): p. 1907-1916.
40. Broz, P., et al., *Differential Requirement for Caspase-1 Autoproteolysis in Pathogen-Induced Cell Death and Cytokine Processing.* Cell Host & Microbe, 2010(6): p. 471.
41. Rathinam, V.A.K., S.K. Vanaja, and K.A. Fitzgerald, *Regulation of inflammasome signaling*.
42. Sahillioglu, A.C., et al., *Structural and Dynamics Aspects of ASC Speck Assembly*.
43. Park, Y.H., et al., *Pyrin inflammasome activation and RhoA signaling in the autoinflammatory diseases FMF and HIDS.* Nature Immunology, 2016. **17**(8): p. 914-921.
44. Thornberry, N.A., et al., *A novel heterodimeric cysteine protease is required for interleukin-1 beta processing in monocytes.* Nature, 1992. **356**(6372): p. 768-74.
45. Gu, Y., et al., *Interleukin-1β converting enzyme requires oligomerization for activity of processed forms in vivo.* EMBO Journal, 1995. **14**(9): p. 1923-1931.

46. Sleath, P.R., et al., *Substrate specificity of the protease that processes human interleukin-1 beta.* The Journal Of Biological Chemistry, 1990. **265**(24): p. 14526-14528.
47. Schechter, I. and A. Berger, *On the size of the active site in proteases. I. Papain. 1967.* Biochemical and biophysical research communications, 2012. **425**(3): p. 497-502.
48. Amor, B., et al., *Uncovering allosteric pathways in caspase-1 using Markov transient analysis and multiscale community detection.* MOLECULAR BIOSYSTEMS, 2014. **10**(8): p. 2247-2258.
49. Luksch, H., et al., *Naturally Occurring Genetic Variants of Human Caspase-1 Differ Considerably in Structure and the Ability to Activate Interleukin-1 beta.* HUMAN MUTATION, 2013. **34**(1): p. 122-131.
50. Walker, N.P.C., et al., *Crystal structure of the cysteine protease interleukin-1beta-converting enzyme: a (p20/p10)2 homodimer.* Cell, 1994(2): p. 343.
51. Stennicke, H.R. and G.S. Salvesen, *Properties of the caspases*.
52. Yang, X., H.Y. Chang, and D. Baltimore, *Article: Autoproteolytic Activation of Pro-Caspases by Oligomerization.* Molecular Cell, 1998. **1**: p. 319-325.
53. Grutter, M.G., *Caspases: key players in programmed cell death*.
54. Datta, D., et al., *Substrate and inhibitor-induced dimerization and cooperativity in caspase-1 but not caspase-3.* Journal of Biological Chemistry, 2013. **288**(14): p. 9971-9981.
55. Thornberry, N.A. and S.M. Molieaux, *Interleukin-1β Converting Enzyme: A Novel Cysteine Protease Required for IL-1β Production and Implicated in Programmed Cell Death*, in *Protein Science*, M.R.L. Department of Enzymology, Rahway, New Jersey 07065 and M.R.L. Department of Molecular Immunology, Rahway, New Jersey 07065, Editors. 1994. p. 3-12.
56. Talanian, R.V., et al., *Stability and oligomeric equilibria of refolded interleukin-1β converting enzyme.* Journal of Biological Chemistry, 1996. **271**(36): p. 21853-21858.
57. Ali, M.H. and B. Imperiali, *Review: Protein oligomerization: How and why.* Bioorganic & Medicinal Chemistry, 2005. **13**: p. 5013-5020.
58. Salvesen, G.S. and V. Dixit, *Caspases: intracellular signaling by proteolysis.* Cell, 1997(4): p. 443.
59. del Sol, A., et al., *The Origin of Allosteric Functional Modulation: Multiple Pre-existing Pathways.* Structure (London, England : 1993), 2009. **17**(8): p. 1042-1050.

60. Gunasekaran, K., B.Y. Ma, and R. Nussinov, *Is allostery an intrinsic property of all dynamic proteins?*
61. Datta, D., et al., *An Allosteric Circuit in Caspase-1.* Journal of Molecular Biology, 2008. **381**: p. 1157-1167.
62. Scheer, J.M., M.J. Romanowski, and J.A. Wells, *A Common Allosteric Site and Mechanism in Caspases*. 2006, National Academy of Sciences. p. 7595.
63. Hardy, J.A., et al., *Discovery of an Allosteric Site in the Caspases*. 2004, National Academy of Sciences. p. 12461.
64. Goldstein, R.C. and A.D. Schwabe, *Prophylactic colchicine therapy in familial Mediterranean fever. A controlled, double-blind study.* Annals Of Internal Medicine, 1974. **81**(6): p. 792-794.
65. Sem, D.S., *NMR-guided Fragment Assembly*, in *Fragment-based Approaches in Drug Discovery*. 2006, Wiley-VCH Verlag GmbH & Co. KGaA. p. 147-180.
66. O'Brien, T., et al., *Structural analysis of caspase-1 inhibitors derived from tethering*.
67. Vandecandelaere, A., S.R. Martin, and Y. Engelborghs, *Response of microtubules to the addition of colchicine and tubulin-colchicine: evaluation of models for the interaction of drugs with microtubules.* Biochemical Journal, 1997. **323**(Pt 1): p. 189-196.
68. Shen, M.-y. and A. Sali, *Statistical potential for assessment and prediction of protein structures.* Protein Science : A Publication of the Protein Society, 2006. **15**(11): p. 2507-2524.
69. Yang, Y.D., et al., *Sub-AQUA: real-value quality assessment of protein structure models.* Protein Engineering, Design and Selection, 2010. **23**(8): p. 617-632.
70. Humphrey, W., A. Dalke, and K. Schulten, *VMD: Visual molecular dynamics.* Journal of Molecular Graphics, 1996. **14**(1): p. 33-38.
71. Phillips, J.C., et al., *Scalable molecular dynamics with NAMD.* Journal of Computational Chemistry, 2005. **26**(16): p. 1781-1802.
72. Meller, J., *Molecular Dynamics*. 2003, Wiley.
73. Liu, Q., Z. Li, and J. Li, *Use B-factor related features for accurate classification between protein binding interfaces and crystal packing contacts.* BMC Bioinformatics, 2014. **15**(Suppl 16): p. S3-S3.
74. Yuan, Z., J. Zhao, and Z.-X. Wang, *Flexibility analysis of enzyme active sites by crystallographic temperature factors.* Protein Engineering, Design and Selection, 2003. **16**(2): p. 109-114.

75. Janowski, P.A., et al., *Peptide Crystal Simulations Reveal Hidden Dynamics.* Journal of the American Chemical Society, 2013. **135**(21): p. 7938-7948.
76. Donald, J.E., D.W. Kulp, and W.F. DeGrado, *Salt bridges: Geometrically specific, designable interactions*. 2011.